UNIVERSIDADE FEDERAL DE MINAS GERAIS
Escola de Engenharia
Programa de Pós-Graduação em Saneamento, Meio Ambiente e Recursos Hídricos

Victor Rezende Moreira

RETROFIT OF CONVENTIONAL DRINKING WATER TREATMENT PLANTS: strategies for arsenic removal improvement

Belo Horizonte
2021

Victor Rezende Moreira

RETROFIT OF CONVENTIONAL DRINKING WATER TREATMENT PLANTS: strategies for arsenic removal improvement

Dissertação apresentada ao Programa de Pós-graduação em Saneamento, Meio Ambiente e Recursos Hídricos da Universidade Federal de Minas Gerais, como requisito parcial à obtenção do título de Mestre/Doutor em Saneamento, Meio Ambiente e Recursos Hídricos.

Área de concentração: Meio ambiente

Linha de pesquisa: Caracterização, prevenção e controle da poluição

Orientador: Drª Míriam Cristina Santos Amaral Moravia

Coorientador: Drª Lucilaine Valéria de Souza Santos

Belo Horizonte
2022

Moreira, Victor Rezende.
M835r Retrofit of conventional drinking water treatment plants [recurso eletrônico]: strategies for arsenic removal improvement/ Victor Rezende Moreira. – 2021.
1 recurso online (90 f. : il., color.) : pdf.

Orientadora: Míriam Cristina Santos Amaral.
Coorientadora: Lucilaine Valéria de Souza Santos.

Dissertação (mestrado) - Universidade Federal de Minas Gerais, Escola de Engenharia.

Apêndices: f. 89-90.
Bibliografia: f. 75-88.
Exigências do sistema: Adobe Acrobat Reader.

1. Engenharia sanitária - Teses. 2. Meio ambiente - Teses. 3. Abastecimento de água – Teses. 4. Membranas (Tecnologia) – Teses. 5. Colóides – Teses. 6. Ultrafiltração – Teses. I. Amaral, Míriam Cristina Santos. II. Santos, Lucilaine Valéria de Souza. III. Universidade Federal de Minas Gerais. Escola de Engenharia. IV. Título.

CDU: 628(043)

Ficha catalográfica elaborada pela Bibliotecária Letícia Alves Vieira - CRB-6/2337
Biblioteca Prof. Mário Werneck - Escola de Engenharia da UFMG

UNIVERSIDADE FEDERAL DE MINAS GERAIS
[ESCOLA DE ENGENHARIA]
COLEGIADO DO CURSO DE GRADUAÇÃO / PÓS-GRADUAÇÃO EM [SANEAMENTO, MEIO AMBIENTE E RECURSOS HÍDRICOS]

FOLHA DE APROVAÇÃO

["Retrofit Of Conventional Drinking Water Treatment Plants: Strategies For Arsenic Removal Improvement"]

[Victor Rezende Moreira]

Dissertação de Mestrado] defendida e aprovada, no dia **[** 17 de agosto de 2021**]**, pela Banca Examinadora designada pelo [Colegiado do Programa de Pós-Graduação **EM SANEAMENTO, MEIO AMBIENTE E RECURSOS HÍDRICOS**] da Universidade Federal de Minas Gerais constituída pelos seguintes professores:

[Prof. Dr. Adriano Aguiar Mendes**] - Membro Externo]**

[UNIFAL]

[Prof. Rubén Dario Sinisterra Millán**] - Membro Interno]**

[UFMG]

[Profª. Drª. Lucilaine Valéria de Souza Santos - **Coorientadora]**

[PUC-MINAS]

[Profª. Drª. Míriam Cristina Santos Amaral Moravia - **Orientadora]**

[UFMG]

APROVADA PELO COLEGIADO DO PPG SMARH

Sonaly Cristina Rezende Borges de Lima - Coordenadora

Belo Horizonte, 17 de agosto 2021.

Documento assinado eletronicamente por **Adriano Aguiar Mendes**, **Usuário Externo**, em 17/08/2021, às 16:18, conforme horário oficial de Brasília, com fundamento no art. 5º do Decreto nº 10.543, de 13 de novembro de 2020.

Documento assinado eletronicamente por **Lucilaine Valéria de Souza Santos**, **Usuário Externo**, em 19/08/2021, às 13:22, conforme horário oficial de Brasília, com fundamento no art. 5º do Decreto nº 10.543, de 13 de novembro de 2020.

Documento assinado eletronicamente por **Miriam Cristina Santos Amaral Moravia**, **Professora do Magistério Superior**, em 19/08/2021, às 13:39, conforme horário oficial de Brasília, com fundamento no art. 5º do Decreto nº 10.543, de 13 de novembro de 2020.

Documento assinado eletronicamente por **Ruben Dario Sinisterra Millan**, **Professor do Magistério Superior**, em 20/09/2021, às 19:20, conforme horário oficial de Brasília, com fundamento no art. 5º do Decreto nº 10.543, de 13 de novembro de 2020.

Documento assinado eletronicamente por **Sonaly Cristina Rezende Borges de Lima**, **Coordenador(a) de curso de pós-graduação**, em 10/11/2021, às 11:58, conforme horário oficial de Brasília, com fundamento no art. 5º do Decreto nº 10.543, de 13 de novembro de 2020.

A autenticidade deste documento pode ser conferida no site https://sei.ufmg.br/sei/controlador_externo.php?acao=documento_conferir&id_orgao_acesso_externo=0, informando o código verificador **0905266** e o código CRC **C8E78231**.

Referência: Processo nº 23072.243013/2021-66 SEI nº 0905266

“Eu aprendi qual é o valor de um sonho alcançar. Entendi que no caminho pedras terão. Eu vi em um universo aberto se erguer ciência, conhecimento e progresso. E foi com muitas pedras. E foi com muitas mãos. Por muitas vezes vi o meu limite vir diante de mim. Enfrentei batalhas que eu não venci, mas o troféu não é só para quem não fracassar. E ao olhar para trás, para tudo que passou, posso agradecer quem comigo estava. Hoje eu sou quem eu sou pois Sua mão me acompanhava. Mas eu sei, não é o fim. É só o começo da jornada. Vejo vitórias se hoje eu olho para trás, e a minha frente eu creio que tem muito mais. Eu sei que minha jornada aqui só começou, e ao longo dessa estrada sozinho eu não estou.”

Só o começo – Vocal Livre (Pedro Valença)

AGRADECIMENTOS

Ser grato não é uma reação ocasional a uma experiência positiva apenas, mas também reconhecer que sobretudo está Aquele que foi, e sempre será, guia e companheiro em todos os momentos. Agradeço a Deus, acima de tudo, pela constante presença.

Aos meus pais João e Maria, e a minha irmã Larissa, por terem me dado a mão nas diversas vezes que ousei sonhar; que nos momentos de dúvida me fizeram entender que o futuro é feito a partir da constante dedicação ao presente.

A minha orientadora Drª Míriam Cristina Santos Amaral Moravia, e coorientadora Drª Lucilaine Valéria de Souza Santos, por transmitirem uma das maiores virtudes que adquiri nesses últimos anos: o conhecimento. Meu agradecimento a vocês, que em momento algum retiveram para si o poder do saber.

Aos amigos e colegas do Grupo de Estudos e Aplicações de Processos de Separação por Membranas, que fizeram parte das minhas mais expressivas conquistas ao longo desses anos, as quais reconheço que sem vocês não seriam possíveis.

Ao Programa de Pós-graduação em Saneamento, Meio Ambiente e Recursos Hídricos da UFMG, pela oportunidade. A Fundação de Amparo à Pesquisa do Estado de Minas Gerais – FAPEMIG, pela concessão de recursos. Ao Conselho Nacional de Desenvolvimento Científico e Tecnológico – CNPq, pela concessão de recursos. A Coordenação de Aperfeiçoamento de Pessoal de Nível Superior – CAPES, pela concessão de recursos.

RESUMO

Um abastecimento seguro de água potável depende da eficácia das estações de tratamento em remover os contaminantes da água bruta, entre eles o arsênio. Com este intuito, um módulo de ultrafiltração submerso (UFs) foi integrado ao processo convencional de tratamento de água (pré-oxidação, coagulação-floculação, decantação e filtração em areia) como estratégia de controle a remoção arsênio. Diferentes condições turbidez (controle, 300 e 1000 NTU) e concentrações de arsênio (0,015 - 0,4 mg/L) foram consideradas, além da interferência do ferro e manganês. Os processos convencionais se demonstraram altamente dependentes das características físico-química da água bruta. Os resultados reforçaram a limitação dos processos convencionais para atingir os valores preconizados em legislação para arsênio e manganês, problema superado pela implantação da UFs (C_{As}: <5 µg/L; C_{Mn}: <0,1 mg/L e C_{Fe} < 0,08 mg/L). Uma análise econômica sensitiva demonstrou que a implantação da UFs torna-se mais atrativa em instalações de maior capacidade de tratamento. Conforme a capacidade de tratamento aumenta (0,108 - 12.690 m³/h), os custos operacionais reduzem (0,98 - 0,81 US$/m³). Uma segunda estratégia combinou os processos de pré-oxidação e membranas de osmose reversa reciclada (UFr), cuja eficiência foi comparada com membranas comercialmente disponíveis. A pré-oxidação promoveu a conversão de espécies solúveis em coloides e complexos que foram posteriormente removidos pelas unidades ultrafiltração mesmo em condições de alta turbidez (1000 NTU). A UFr foi capaz de reter até mesmo os complexos de menor diâmetro equivalente, sendo o único sistema capaz de atingir os valores limite para os três contaminantes. Apesar do menor fluxo de permeado e menor vida útil associado à UFr, o processo apresentou o menor custo operacional (0,310 US$/m³) e maior taxa de retorno em comparação com as outras configurações. As vantagens da UFr podem ser estendidas a outros aspectos ambientais, pois diminui o descarte de membranas em fim de vida em aterros e, ao mesmo tempo, atinge os pré-requisitos técnicos e econômicos para novas tecnologias que se buscam para um abastecimento de água potável. Os resultados ainda sugerem que os módulos de ultrafiltração podem contribuir para um abastecimento seguro de água potável.

Palavras-chave: Tratamento de água potável; Membranas; Abastecimento de água; Membranas recicladas; Ultrafiltração

ABSTRACT

A safe drinking water supply relies on the efficiency of drinking water facilities to remove the contaminants from raw surface water, among them arsenic. At first, dead-end ultrafiltration (UFs) was integrated to a conventional drinking water treatment process (pre-oxidation, coagulation-flocculation, decantation, and sand filtration) as a strategy for arsenic control in drinking water. Different turbidities (control, 300 and 1000 NTU) and arsenic concentration (0.015 – 0.4 mg/L) were considered, in addition to the interference of iron and manganese. Conventional treatment processes were highly dependent on surface water quality, although the removal of colour and turbidity seems not to be a major concern. The results reinforced the limitation of the conventional treatment process for attaining the threshold values especially for arsenic and manganese, an issue overcame by the implementation of an UFs (C_{As}: <5 µg/L; C_{Mn}: <0.1 mg/L e C_{Fe} < 0.08 mg/L). A sensitive analysis demonstrated that the implementation of a UF becomes more economically attractive in facilities with a greater treatment flow rate. As the treatment capacity increased (0.108 – 12,690 m³/h) the operating costs decreased (0.98 – 0.81 US$/m³). A second strategy combined a pre-oxidation process and recycled reverse osmosis membranes (UFr), which efficiency was compared with commercially available UF membranes. The pre-oxidation employed was effective in converting soluble species into colloids and complexes that were later removed by ultrafiltration units even under high turbidity conditions (1000 NTU). The UFr was capable to retain even the complexes of smaller equivalent diameters, being the only system capable to attain the threshold values for all three contaminants. Despite the lower permeate flux and shorter membrane lifespan for UFr, the process still presented the lowest operating cost (0.310 US$/m³) and the highest rate of return compared to the other configurations. The advantages of UFr could be extended to environmental aspects as diminishes the disposal of end-of-life membranes in landfills whilst attaining the technical and economical pre-requisites for novel technologies being sought for a safe drinking water supply. Moreover, the results suggested that ultrafiltration can be used to retrofit drinking water treatment plants, guaranteeing a safe drinking water supply.

Keywords: Drinking water treatment; Membranes; Colloids; Safe water supply; Recycled membranes; Ultrafiltration

LIST OF FIGURES

LIST OF TABLES

LIST OF ABBREVIATIONS, VARIABLES AND SYMBOLS

Ap. C	Apparent colour (uH)
C/F	Coagulation-flocculation
CapEX	Capital expenditure
$C_{As,0}$	Initial arsenic concentration (mg/L)
CEPCI	Chemical engineering cost index
CF	Coagulation-flocculation
$C_{Fe,0}$	Initial iron concentration (mg/L)
$C_{Mn,0}$	Initial manganese concentration (mg/L)
CT	Conventional treatment
EC	Electrical conductivity (µS/cm)
J/J_0	Permeate flux decay
k_c	Mass transfer coefficient correlated to complete blocking (1/s)
k_{cl}	Mass transfer coefficient correlated to cake layer formation (s/m^2)
k_i	Mass transfer coefficient correlated to intermediate blocking (1/m)
k_s	Mass transfer coefficient correlated to standard blocking ($1/m^{0.5}s^{0.5}$)
MSPs	Membrane separation processes
NPV	Net present value
OpEX	Operating expenditure
$P_{25\%}$	Percentil 25%
$P_{75\%}$	Percentil 75%
R_{As}	Arsenic removal after coagulation-flocculation (%)
R_{Fe}	Iron removal after coagulation-flocculation (%)
R_{Mn}	Manganese removal after coagulation-flocculation (%)
RO	Reverse osmosis
RoR	Rate of return
SF	Sand filtration
Turb	Turbidity (NTU)
UF	Ultrafiltration
UFp	Pressurized ultrafiltration
UFr	Recycled reverse osmosis membrane
UFs	Submerged ultrafiltration
WHO	World health organization
WS_i	Water sample “i”
Z	Man-Whitney statistics
χ^2	Chi-square statistics

TABLE OF CONTENTS

CHAPTER 1

THEORETICAL BACKGROUND

MOREIRA, V. R. et al. Arsenic contamination, effects and remediation techniques: A special look onto membrane separation processes. **Process Safety and Environmental Protection**, 2020. DOI: 10.1016/j.psep.2020.11.033

1.1 INTRODUCTION TO CONVENTIONAL DRINKING WATER TREATMENT PROCESSES

Arsenic is a naturally occurring metalloid whose presence in environmental matrices can be intensified due to anthropic activities. For instance, weathering, biological and volcanic activity, along with anthropogenic activities (such as mining, fossil fuels burning, pesticide and herbicide application, and crop desiccants) are the main responsible for the high concentration values reported in Figure 1. In South America, Brazil included, concentrations ranging from 0.009 up to 1,660 µg/L were previously documented in recent research papers [1]. Environmental arsenic contamination is not a localized issue, neither restrained to short-income countries, and deserves special attention given the human health impacts related to its ingestion. Besides the direct consumption of contaminated drinking water, the main pathways for human exposure to arsenic are via consumption of contaminated food and inhale of dust and fumes.

The results summarized in Figure 1 evidence that concentrations above the threshold for drinking water (10 µg/L, from World Health Organization) are indeed a subject that must be paid attention. The drastic reduction of the reference value from 50 to 10 µg/L in 1993 has led to an increase in research and development of drinking water facilities, which have undergone several technical and operational improvements induced by their non-compliance of arsenic levels. Alongside arsenic, iron (concentration range: 0.31 – 50 mg/L) and manganese (concentration range: 0.48 – 1.5 mg/L) are often ubiquitous ions as all three species generally derive from the same rocky matrix [2,3]. Iron is usually found in natural, surface and underground waters, as insoluble and dissolved species, such as oxides, silicates, carbonates, chlorides, sulfates, and sulfites. Manganese is also present as dissolved and insoluble compounds, although in lower concentrations compared to iron [3,4].

While there is no evidence of toxicity associated with iron, the human health impact related to short- and long-term exposure to arsenic and manganese is well established. For arsenic, the impacts include effects over the respiratory system [5–8], hepatic system [9–12], neurological system [13–16], renal system [5,17,18], reproductive system [19,20], in addition to mutagenetic [21,22] human health effects. The ingestion of high levels of manganese, in its turn, can affect neurological development and

behavior; provoke deficits in memory, attention, and motor skills, especially in children [23,24]. In addition, the presence of iron and manganese in water provides undesirable aspects such as changes in color, odor, astringent bitter taste, and increased turbidity, leading to rejection by consumers.

Figure 1. Worldwide arsenic distribution in surface and groundwater. Reference: [1]. Note: y-axis represented in a log scale.

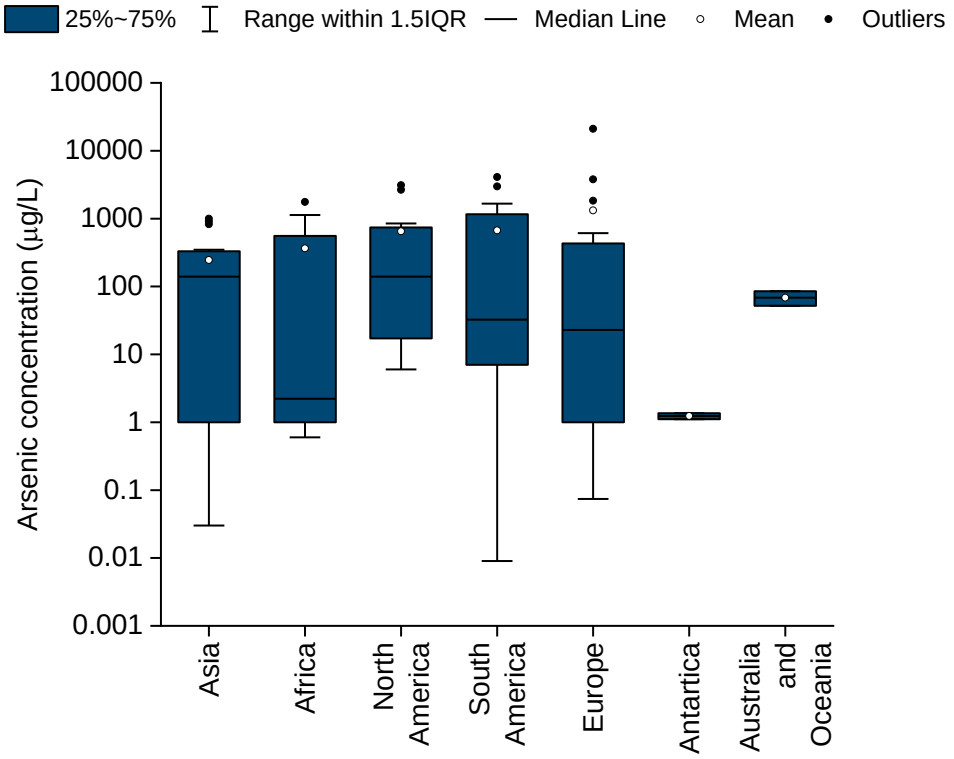

The removal of arsenic, iron, and manganese from surface water is highly dependent on the water physicochemical characteristics, and the conventional physical-chemical processes as coagulation-flocculation, decantation, and sand filtration are often ineffective in achieving the threshold values drinking water, especially in terms of arsenic and manganese [25]. These processes are represented in Figure 2 and will be detailed in the following sections, along with strategies and technologies currently under development intended for higher efficiency of arsenic, iron, and manganese removal.

Figure 2. Representation of conventional treatment processes applied for drinking water obtainment.

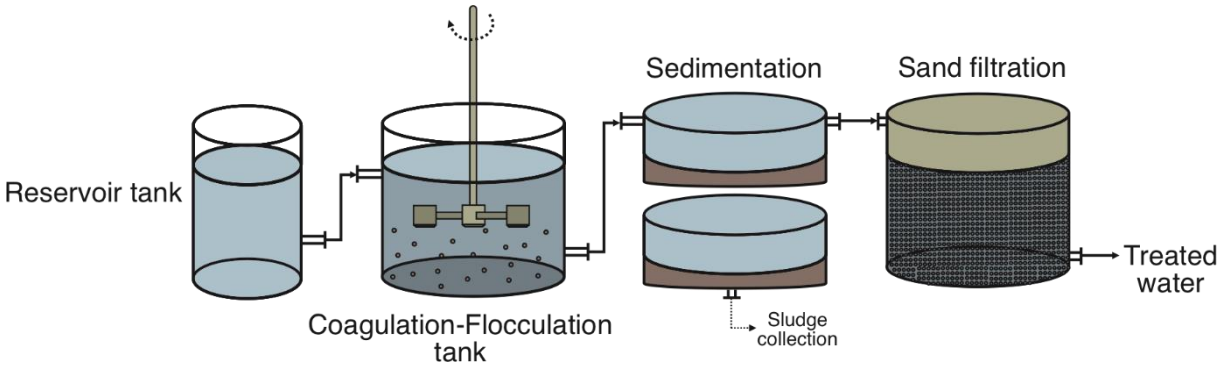

1.1.1 Coagulation-flocculation

Precise control of the coagulation-flocculation processes is required for reasonable performance of conventional drinking water treatment plants (DWTPs). The coagulant is initially dosed to a reservoir tank or raw water stream, and a rapid mixing stage is employed for its dispersion (coagulation stage). Following that, different and lower mixing rates are employed intend to transform impurities in fine suspension into larger flocs or flakes (flocculation stage), later removed by settling tanks, filtration, and in some cases flotation. Different variables interfere in coagulation-flocculation processes starting the water physicochemical characteristics, but also the coagulant agents, their dosage, the water pH, temperature, mixing rate, and mixing time [26,27]. In systems with a high concentration of colloidal particles, these particles approach and collide with each other due to continuous and disordered movements (Brownian movement), interacting by their diffuse layers through van der Walls forces or repulsion due to electrostatic or electrical double layer forces [28].

Coagulation results from the action of four distinct phenomena, namely, diffuse layer compression, adsorption and charge neutralization, sweeping, and bridging or patch flocculation. Before their definition, it is necessary to conceptualize the electric double layer. Colloids and suspended particles are predominantly negative and attract part of the positive ions (positive) in the solution that tightly bounds around its surface. This first layer formed is referred to compact layer or Stern layer. When negative ions approach the compact layer, they attract positive ions with them which results in the diffuse layer. The set of layers, compact and diffuse, is what is defined as an electrical double layer (Figure 3). In a stable colloidal suspension scenario, the repulsive forces

exerted by the electric double layer predominate over a certain distance range (DLVO theory). Its destabilization is the main purpose of coagulation processes, and one of the ways to achieve that is to promote the diffuse layer compression [26,27].

Figure 3. Double electric layer representation in a stabilized colloidal suspension.

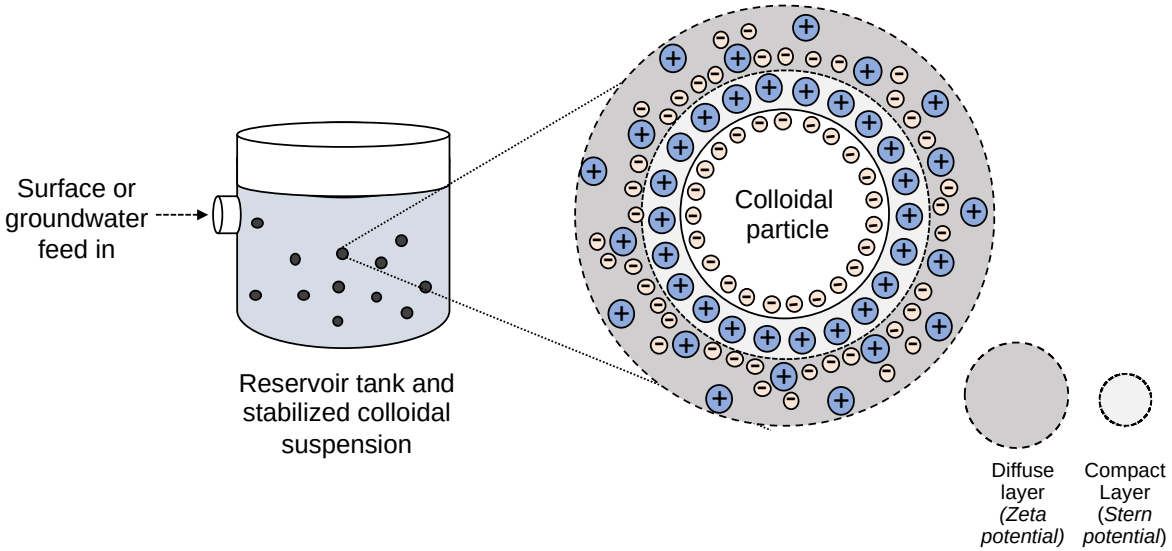

Diffuse layer compression is caused by the addition of positive ions, opposite to that of the colloidal particles. The greater the ion charge, the smaller is the amount required for coagulation. After introduced to the medium, the electrolytes will cause an increase in the density of positive charges in the diffuse layer, which reduces its sphere of influence to remain electrically neutral. As a result, the particle's electrical potential is reduced and van der Walls forces prevail. Dealing with diffuse layer compression, it is worth mentioning two aspects. The first one concerns the number of electrolytes needed to achieve coagulation, which is considered practically independent of the colloids' concentration in the water. The second aspect points to the fact that it is not possible to reverse the colloids charge (promote the colloidal suspension re-stabilization) regardless of the amount of the electrolyte added [29]. This mechanism is characterized by large metal ions concentrations to achieve destabilization, which makes it impractical for water treatment [26].

The phenomenon of adsorption and charge neutralization derives from interactions between the coagulant-colloid, coagulant-solvent, and colloid-solvent. In this case, the colloidal suspension destabilization occurs by adsorption of species with opposite

charge onto the colloids' surface [29,30]. The coagulant amount required to promote colloids destabilization is lower when compared to requirements for diffuse layer compression. In addition to this fact, there is a stoichiometric relationship between the colloids and coagulant concentrations and it is possible to reverse the colloidal particles' surface charge increasing the dose of adsorbable species. This mechanism is generally considered for water treatment processes that employ direct filtration. For these systems, there is no need for flocks formation since the destabilized particles would be retained by the filtering medium [29].

The sweeping occurs by precipitates formation (*e.g.*: iron or aluminum hydroxides, depending on the coagulating agent) and is conditioned by the amount of coagulant, medium pH, and concentration of other ions in the water. Such precipitates involve the colloids, which are not necessarily neutralized and/or destabilized, and provide for the formation of flocs with greater density and therefore settling rate. The mechanism is widely used in conventional DWTPs accounted with flocculation, sedimentation, and filtration processes. Finally, bridges and patch flocculation are related to the use of organic compounds (polymers), synthetic or natural, as coagulants. Such polymers adsorb the colloidal particles in ionizable sites that compose their chains, also forming flakes that will be later removed by sedimentation and sand filters [29].

Currently, there is a variety of coagulant agents employed in full-scale facilities and other still under development, classified as chemical and natural agents. The decision for the most suitable coagulant must consider its efficiency, chemical requirements for its proper performance, residual sludge produced, and costs [31].

Among the coagulants commercially available, iron- and aluminum-based chemicals are widely used in DWTPs given their favorable cost-benefit ratio. Iron salts are effective over a wide pH range, removing colour at low pH values and iron and manganese at high pH values [28,31]. According to several authors [28,29,31,32], ferric chloride has been successfully used in a large number of DWTPs, operating at higher pH ranges than aluminum sulfate and preferred for the treatment of highly coloured waters. This coagulant produces heavier flocs with greater settling rates compared with flocs formed with aluminum salts and can oxidize substances

responsible for undesired taste and odor. Iron salts still stand out from aluminum salts, since the extensive use of aluminum-based agents can lead to high residual concentrations of aluminum in treated water, whose impact on human health has already been proven by recent studies [33,34].

More recently, natural coagulants have been studied for water treatment; however, as evidenced by Ang & Mohammad [35], their widespread application in DWTPs is still low. Examples of natural coagulants are chitosan, cellulose, tannin-based agents, and starch. The same authors pointed out the necessity of studies that investigates strategies to enhance their performance as coagulants, proves their compatibility with other treatment technologies in integrated/hybrid treatment process, verify the possibility of hybridizing natural coagulants with other types of coagulants; improve the extraction and purification efficiency for the obtainment of high purity coagulants, and the synthesis of multifunctional natural coagulants [35].

The state-of-art also points to different coagulation techniques. Despite their greater efficiency, their application is still limited to lab-scale studies. Lv et al. [36] investigated the magnetic seeding coagulation-flocculation process for surface water treatment. The technology has been used to accelerate flocs sedimentation with an applied magnetic field, offering large handling capacity and low energy consumption. Studies have also considered the recovery of magnetic particles from flocs with an applied magnetic field [37], leading to a reduced volume of sludge to be further disposed. Other technologies being developed are electrocoagulation [26] and hybrid configurations as coagulation-flocculation-adsorption [38] and coagulation-flocculation-membranes filtration [39].

Following coagulation, flocculation is occurs by different mixing gradients responsible to promote contact between the destabilized colloids and intends to obtain visible suspended particles. There are three main mechanisms responsible for an effective flocculation. Perikinetic flocculation, resulting from Brownian motion provided by the fluid thermal energy, orthokinetic flocculation, predominant in water treatment in which the particles are brought into contact through the fluid movement (different velocity gradient) and flocculation by differential sedimentation, in which particles with different

velocities can collide with each other in an element volume. [28,29]. The flocs formed have a greater density and higher settling rate and allows for a liquid-solid separation by settling, flotation, or filtration units.

1.1.2 Sand filtration

Sand filters are used as an additional barrier to suspended materials that remained in the water after coagulation-flocculation. The structures could be filled with sand of different granulometry depending on its purpose, and the suspended material is captured by different mechanisms: direct collision, van der Walls attraction forces, electrostatic attraction, or even diffusion [31]. The predominance of one or more of these mechanisms depends on the sand-bed particle size distribution, sand-bed porosity, and filtration rate. In summary, the removal of particulate and colloidal species of arsenic, iron, and manganese could occur by a physical barrier promoted by the filters, whereas their dissolved species are removed, in a lower extension, by adsorption. The distribution of arsenic, iron, and manganese, according to the surface water pH is shown in Figure 4.

In conditions close to which surface waters are found (pH 5.5 – 7.5, redox potential: ~350 mV and temperature: ~25°C), most arsenic species are found in their pentavalent protonated form. For that reason, these species are removed mainly by electrostatic interactions and with greater efficiency compared to arsenic three [As(III)] species, which are neutral under such conditions. Iron species are mostly distributed in insoluble complexes (therefore removed by physical retention mechanisms), with low contributions of dissolved species to the total iron concentration, and manganese is commonly found at its protonated divalent species. They (Mn^{2+}) are thermodynamically more stable compared to other manganese species and manganese complexes, when formed, have a smaller equivalent diameter than sand filter pores. For this reason, conventional processes can present low manganese removal efficiency. Considering the removal of dissolved species and an adsorption phenomenon, it is also important to consider a phenomenon of competitiveness between the ions of arsenic, iron, and manganese for the sand filter active sites.

Figure 4. Speciation diagrams for (a) arsenic, (b) iron, and (c) manganese. Notes: species of reference: [As(OH)$_3$]TOT, Fe^{2+}, and Mn^{2+}. Temperature: 25 °C. Eh: 0.35 mV.

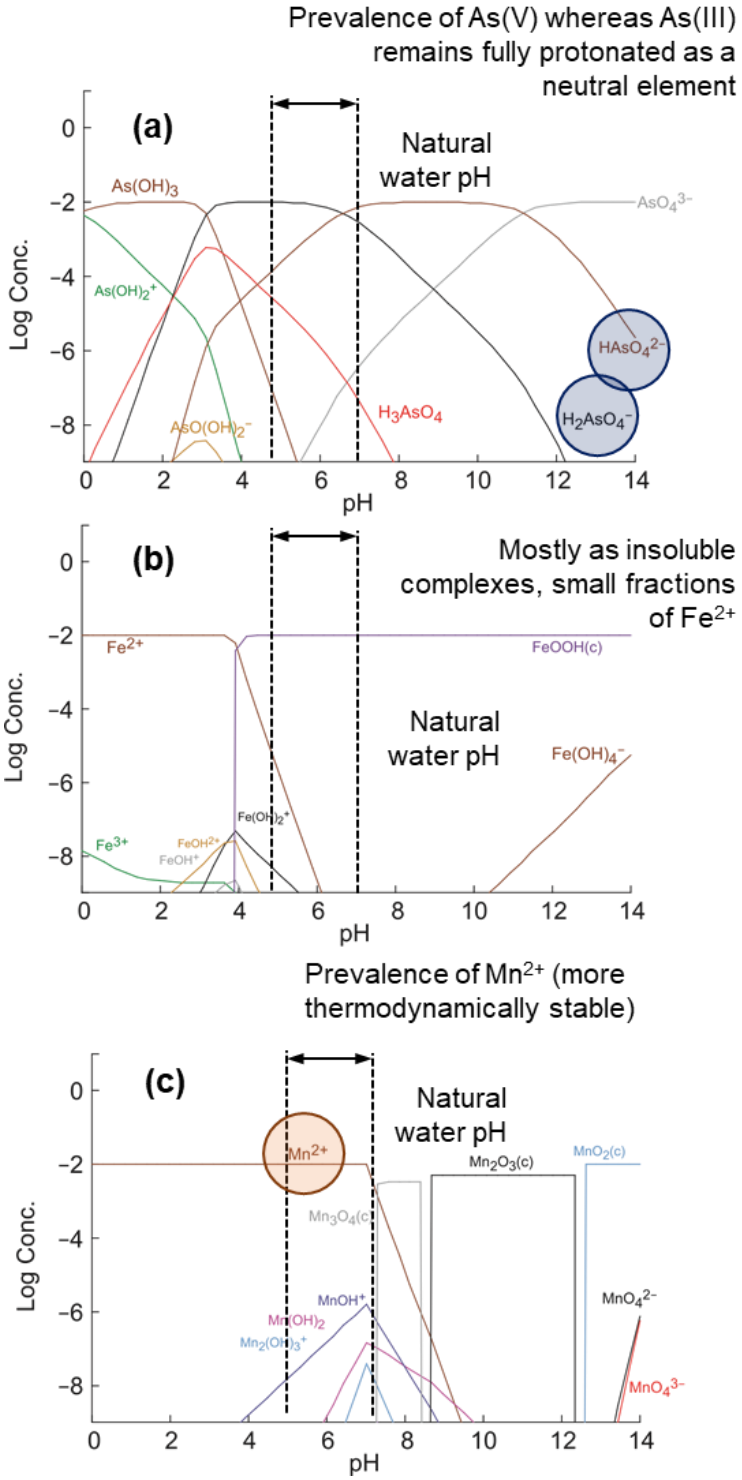

Sand filters can operate either with downward or upward flow, under the action of gravity or pumps, classifying the filtration process as rapid and slow. In both cases, two aspects affect the filter's efficiency and are worthy to be mentioned [31,40]. The

ripening process dictates that the filter efficiency increases as it captures suspended particles. In some cases, the filter effluent may not meet the quality criteria during ripening, and it is necessary to reintroduce the filter effluent to the treatment process [40]. Filter regeneration is another important aspect to be mentioned. The procedure should be adopted whenever noticed a loss in filtration efficiency (usually monitored by residual turbidity and colour values). Through backwashing, particles adhered to the sand grains are removed and the filter-bed can be reused. For backwashing, it is possible to use either water only, or water combined with air [40].

More recently, it has been observed that sand filters are also effective in removing residual iron and manganese, however, conditioned to the presence of manganese-oxidizing bacteria (*e.g.*: *Pseudomonas sp*.) in the filter medium [41,42]. The development of a bacteria culture, though, is not straightforward and requires a certain operation time. In the study presented by Guo et al. [43], the contribution of biological activity for iron and manganese removal was only noticed after two months of operation. The effectiveness of sand filters allows them to be applied for different purposes, including water treatment but also as a pre-treatment for ultrafiltration (UF) systems. Although used to a lesser extent, UF membranes have greater efficiencies in removing high molecular weight compounds and biological indicators [44], with potential for integration with conventional treatments as a form of potable water polishing. Guo et al. [43] coupled continuous sand filtration as a pre-treatment to UF membranes for drinking water treatment. As reported, sand filtration contributed to the obtainment of a permeate with greater physicochemical quality and alleviated the UF membrane fouling.

1.1.3 Strategies to improve arsenic removal and research hypothesis

Apart from being widely spread technologies, coagulation and flocculation depend on several operating variables not often controlled in DWTPs. That would demand a robust monitoring system and constant maintenance measures while treating contaminated water. In terms of arsenic, manganese and iron, the instability in the treatment performance is mainly associated with the limitation in the removal of their colloidal and sub-colloidal particles [31], as well as their dissolved fraction. Recently, Sorlini *et al.* [45] surveyed 19 full-scale DWTPs for their efficiency on arsenic removal

and compliance with the threshold values recommended by the World Health Organization. Apart from those facilities that accounted with advanced treatment processes for potable water polishing (*e.g.*: reverse osmosis and granulated activated char), the limit of 10 µg/L in drinking water was disrespected for all other DWTPs.

Two hypotheses were investigated to improve arsenic removal and were summarized in Figure 5.

Figure 5. Strategies for improving arsenic removal from surface water by conventional drinking water facilities.

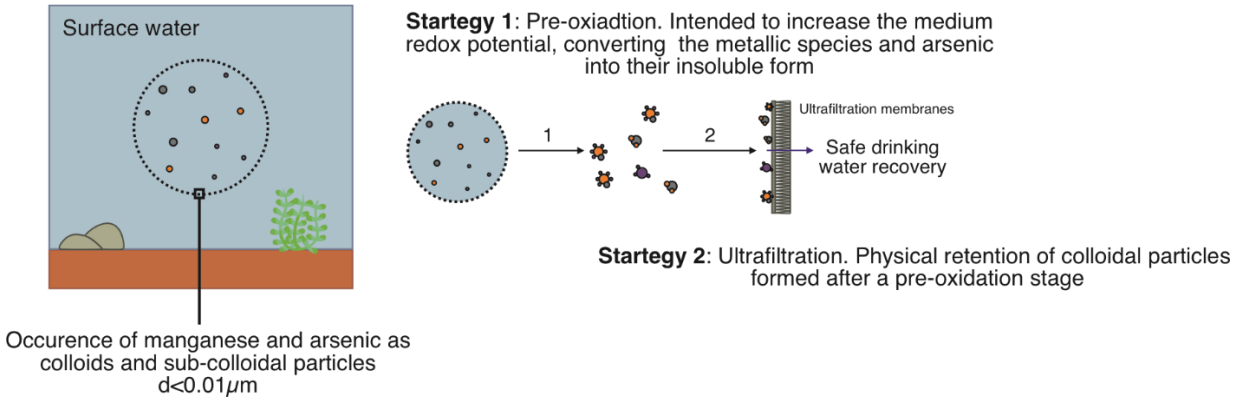

A first hypothesis to increase arsenic removal by conventional treatment process could be the use of a pre-oxidation stage before the coagulation-flocculation. The pre-oxidation procedure is intended to increase the medium redox potential, converting the metallic species and arsenic into their insoluble form [46]. In cases of a real drinking water treatment, a pre-oxidation procedure still converts arsenic (III), which has a poor mineral surface affinity, into arsenic(V) that readily adsorbs to solid surfaces [1,47]. Although the oxidant requirements can be calculated through stoichiometric reactions, experiments must be carried out due to the presence of interfering substances as iron, manganese, sulfide (HS^- and S_2^-), and total organic carbon in water samples. Based on that, it is presumable to assume that an effective pre-oxidation process is still subjected to the surface water characteristics, although in a lower extent, which requires a constant adjustment of the oxidant dosage. In the hypothesis that this adjustment is not always well-performed in drinking water facilities, a more robust alternative may be anticipated [48].

The success of different technologies, including pre-oxidation, coagulation-flocculation, adsorption and ion exchange, and membrane separation processes, have been recently summarized by Moreira *et al.* [1] in an attempt to cover different processes currently employed for arsenic control in drinking water. Among them, the membrane separation processes (MSPs) are recognized for their effectiveness in surface water treatment, either as a pretreatment, standalone or in a conjugated treatment trail [49–53]. Due to their structure and composition, membranes have different morphology (pore size, porosity, hydrophobicity, roughness, and thickness) and separation (permeability and selectivity) characteristics. Ideally, they may present: (i) chemical and mechanical resistance; (ii) high permeability and selectivity; (iii) high durability; and (iv) low cost. From all MSPs commercially available, UF membranes have been effectively applied at both pilot and full-scale installations. Since size exclusion is the main mechanism responsible for pollutants retention by UF membranes, it is not expected an efficient removal of dissolved species of arsenic unless coupled with other processes. That is the case reported by Ahmad et al. [54], which achieved arsenic concentrations lower than 1 µg/L in a combined UF and coprecipitation process with iron (oxyhydr)oxides. The idea of iron oxides favoring arsenic removal depicts real conditions considering that arsenic is mainly found as bearing iron(III) minerals [2,55] and the natural colloids and those formed after pre-oxidation are in the colloid size range (0.001 - 1 µm) [46,56,57]. Thus, although not expected to be removed by the conventional treatment system, more specifically the sand filtration, the colloids formed should be removed without major difficulties by UF (pore size <0.2 µm).

UF modules are currently found in different configurations, most manufactured by hollow fiber membranes. These modules have the highest packing density (~10.000 m^2/m^3) among all modules available, in addition to lower acquisition and operational costs, however poor hydrodynamics [58]. The efficiency of UF membranes for pollutants retention were summarized in Figure 6. There are two primary types of UF modules, submerged (UFs) and pressurized (UFp), differing mainly from their operation mode, but also permeate flux and costs related to their acquisition and operation [59]. UFs has been widely used for water and wastewater treatment based on their lower energy consumption [60] compared to UFp and other membrane

separation processes. UFp, in its turn, has generally higher permeate flux [59,60], a favorable aspect that should be taken into account while deciding on the most cost-effective alternative. Still, these are modules that could present a membrane cost of 980 US$ per unit, which summed up to their cost for annual replacement could represent an investment cost of 1,176 US$ per module [61]. Based on that, de Paula & Amaral [61] proposed the conversion of end-of-life reverse osmosis (RO) membranes into ultrafiltration-like membranes by means of its chemical oxidation. According to the authors, the recycled RO membrane (UFr) would present a membrane cost of 8.53 US$ per unit, besides the environmental gains related to the reuse of a spent membrane. Its effectiveness for surface water treatment in terms of water permeability and salinity rejection has been previously assessed by de Paula et al. [62], and their use for arsenic, in addition iron and manganese, removal seems to be a promising alternative.

Figure 6. Representation of retention efficiency for ultrafiltration membranes.

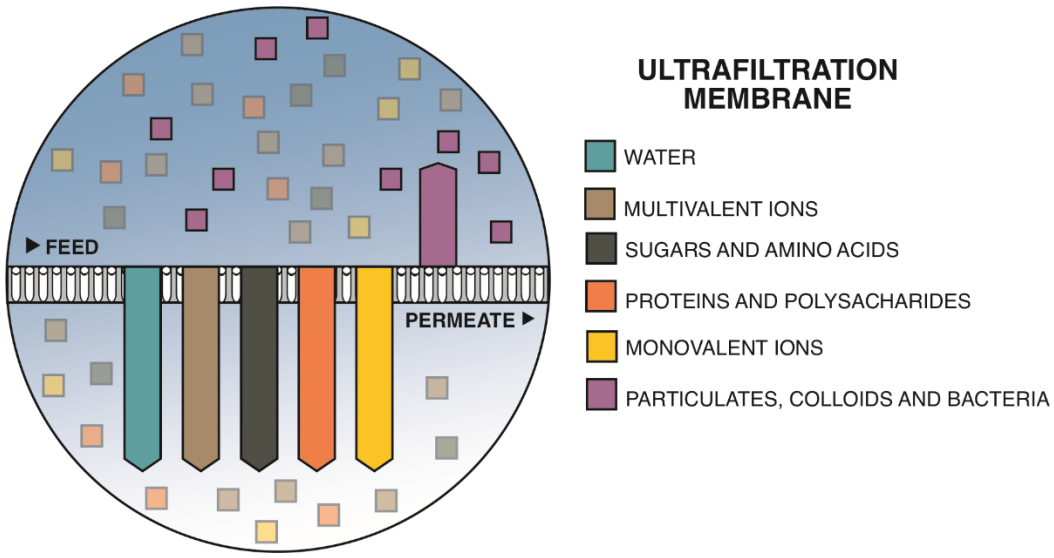

Despite their advantages, UF units are still subject to fouling and scaling, which ultimately affects the permeate flux, membrane integrity, and contaminants removal efficiency. The scenario could be aggravated under high concentrations of suspended solids, leading to irreversible fouling formation over the membrane surface, a key question that remains and deserves a better comprehension while dealing with MSPs.

1.2 Objectives

1.2.1 General objective

Analyze the efficiency of conventional water treatment processes for arsenic removal and the contribution of pre-oxidation and ultrafiltration processes as strategies for retrofitting water treatment plants and a safe drinking water supply.

1.2.2 Specific objective

a) Estimate the overall efficiency of the conventional treatment process (coagulation-flocculation, sedimentation, and sand filtration) for arsenic removal and the interference of iron and manganese;
b) Assess the contribution of a conventional dead-end UF as an additional step for improving arsenic removal in conventional drinking water facilities;
c) Estimate the capital and operational expenditures for the implementation of a UF in conventional drinking water facilities at different treatment capacities;
d) Compare the conventional treatment process with different UF configurations (submerged, pressurized, and recycled reverse osmosis membranes), preceded by a pre-oxidation process, in terms of arsenic removal in the presence of iron, manganese and aluminum;
e) Compare the economic feasibility of different routes (pre-oxidation combined with different UF-like membranes) for their operating and capital expenditures, payback period, rate of return, and net present value.

1.3 Document structure

This master thesis is divided into 5 chapters organized as research papers: Chapter 1 is an introduction and theoretical background, and contains the objectives and the document structure; Chapter 2 addresses specific objectives (a) to (c) whereas Chapter 3 comprehends the investigation of different UF-like membranes combined with a pre-oxidation stage as an alternative treatment route for contaminated surface water treatment [objectives (d) and (e)]. Finally, Chapters 4 and 5 contain the final considerations and references, respectively.

CHAPTER 2

DEAD-END ULTRAFILTRATION AS A COST-EFFECTIVE STRATEGY FOR IMPROVING ARSENIC REMOVAL FROM HIGH TURBIDITY WATERS IN CONVENTIONAL DRINKING WATER FACILITIES

MOREIRA, Victor Rezende et al. Dead-end ultrafiltration as a cost-effective strategy for improving arsenic removal from high turbidity waters in conventional drinking water facilities. **Chemical Engineering Journal**, p. 128132, 2020. DOI: 10.1016/j.cej.2020.128132

1.5 Introduction

Due to the unaffordable costs related to advanced water treatment, a safe drinking water supply in short income countries relies on the efficiency of traditional drinking water treatment facilities, which comprises a coagulation-flocculation stage, followed by sand filtration and disinfection. These processes, however, are often unable to achieve the threshold values for arsenic in drinking water established by the World Health Organization (10 µg/L) [63,64].

Arsenic can be found associated with dissolved organic matter and other metals in the colloid size range (0.001 - 1 µm) [46,56,57]. Bauer & Blodau [46] showed that the distribution of arsenic was mainly on the colloidal form in experimental solutions rich in ferric iron, dissolved organic matter, and arsenic. Especially when an arsenic and iron mixture was considered, about 50% of the arsenic was recovered in particle fraction >0.2 µm. Thus, although not expected to be removed by the conventional treatment system, more specifically the sand filtration, it should be removed without major difficulties by UF (due to its pore size being less than 0.2 µm). For the remaining dissolved fractions of arsenic (<5 kDa), other approaches are required. One alternative is the implementation of the pre-oxidation step so that the arsenic(III) is converted into arsenic(V), which favors precipitates formation [65]. Nevertheless, pre-oxidation processes are conditioned to the surface water composition, and the complexes formed may be unstable. Therefore, their removal would require more robust alternatives.

Membrane separation processes are recognized for their robustness and effectiveness in surface water treatment [66,67]. Pressure-driven processes such as ultrafiltration (UF) have been effectively applied, either as a separate process or integrated with other membrane techniques, at both pilot and full-scale installations. The current Chapter brings an overview of conventional drinking water treatment efficiency on arsenic removal, and the use of dead-end ultrafiltration as strategies to guarantee a safe drinking water supply. In a dead-end configuration, the UF operates in a semicontinuous mode with intermittent backwash, often combined with air scour either during filtration and/or backwash cycles, in which the concentrate is periodically discharged.

Different from a crossflow configuration, dead-end ultrafiltration has the following advantages: (i) all the source water passes through the membrane which leads to a higher recovery rate within a filtration cycle, and (ii) it can handle higher volumes of water. Still, and as evidenced out by Pascual-Benito et al. [68], little is known about the dead-end UF performance in environmental samples with different characteristics or samples under natural conditions.

A pre-oxidation stage was considered before the conventional coagulation-flocculation process, which was followed by sand filtration and UF. In that case, fouling and permeate flux decay would not represent a major concern for dead-end filtration modules as the UF would be treating water with a low concentration of suspended solids, previously removed by sand filtration. Surface waters of different turbidities were simulated considering that surface water quality would affect the overall process efficiency in arsenic removal [54]. Conditions of high-turbidity water are commonly observed along rainy seasons, representing a challenge for water treatment facilities and implications for a safe-drinking water supply [69]. Although turbidity does not necessarily imply a direct risk to public health, the suspended solids responsible for turbidity can serve as a carrier to arsenic, metal ions, and microbial pathogens in surface water samples [69,70].

Based on that, the removal efficiency was assessed at different turbidity and arsenic concentrations for a better comprehension of the limitations faced by drinking water treatment plants in both pollutants control. Ultimately, it was investigated the economic feasibility of the process to assure that the implementation of an additional UF process would be economically viable.

1.6 Material and methods

1.6.1 Surface water sampling and characterization

Surface water and sediments were collected from a local river site that serves as a water source for 51 municipalities (~4.5 million inhabitants). Considering the most recent monitoring study available for the corresponding river [71], seventy-five percent of the arsenic concentration values would be greater than 0.015 mg/L ($P_{25\%}$) and lower than 0.4 mg/L ($P_{75\%}$), which were defined as the spiking limits in the current study (spiked with $Na_2HAsO_4.7H_2O$). Iron ($FeCl_3$) and manganese ($MnSO_4.H_2O$) were also

spiked in surface water to depicts real contaminated conditions. These metals frequently occur concomitantly with arsenic in concentrations ranging from 0.13 – 50 mg/L for iron and 0.48 – 1.5 mg/L for manganese [2,3,72]; therefore, their interference in overall process efficiency was also taken into account. Once collected, the water samples were stored in the absence of light at temperatures below 4 °C and brought to room temperature before their use and characterization. The surface water was characterized in terms of its physicochemical properties, according to the Standard Methods for The Examination of Water and Wastewater [73]. Iron, manganese, and arsenic concentration values were determined by inductively coupled plasma mass spectrometry (ICP-MS; method 3125B; lower quantification limits: 0.001 mg/L).

The particle size distribution of the sediments was measured using a Malvern Mastersizer 2000® laser diffractometer. The result is shown in Figure 7, in which the d_{50} was found to be 8.8 µm. Leaching and solubilization tests of the sediments followed the procedure recommended by NBR 10.004:2004 - Annex F [1]. The results showed that the metal concentrations were below the levels recommended for arsenic (<1.0 mg/L), barium (<70.0 mg/L), cadmium (<0.5 mg/L), lead (<1.0 mg/L), chromium (<5.0 mg/L), fluoride (<150 mg/L), mercury (<0.1 mg/L), silver (<5.0 mg/L) and selenium (<1.0 mg/L). Furthermore, the control experiments ran in parallel (sediments with deionized water) showed that the dissolved concentrations for arsenic, manganese, and iron did not exceed 3 µg/L, 20 µg/L, and 40 µg/L, respectively.

Figure 7. Particle size distribution for the sediment used for water turbidity incrementation.

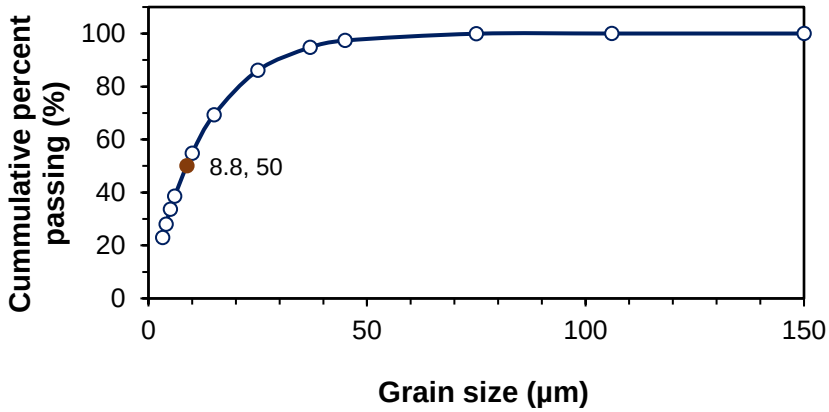

1.6.2 Conventional treatment process

The conventional treatment process comprised a pre-oxidation procedure using sodium hypochlorite (NaOCl), followed by coagulation-flocculation and sand filtration

processes. 2 L of surface water spiked with arsenic, iron, and manganese was pre-oxidized for 1 h in a Jar-test under constant agitation (120 rpm). Prior to coagulation-flocculation, the medium pH was adjusted using a 0.01 mol/L sodium hydroxide (NaOH) or 0.01 mol/L sulfuric acid (H_2SO_4) solution. Iron chloride ($FeCl_3$) was used as a coagulant agent. The paddles were first operated at rapid mixing (100 rpm; 1 min), followed by 68, 44, 37, and 26 rpm all held for 4 min each. The media were left to settle for 5 min (settling velocity: 1.5 cm/s) and the supernatant was collected for physicochemical characterization and further sand filtration. A down-flow sand filtration system was used with a height of 240 mm and inner diameter of 19 mm, filled with conventional sand with an average particle diameter of 0.297 – 1.18 µm (depth: 150 mm). Before each test, the filters were compacted using deionized water (500 mL).

The efficiency of the conventional treatment process was initially assessed considering surface water of different turbidity (1000 and 300 NTU) and fixed concentration of arsenic, iron, and manganese (WS3 in Table 1), which were compared to a control water sample in which there was no turbidity increment. The effect of different arsenic, iron, and manganese concentrations was also assessed, for fixed initial turbidity of 1000 NTU. A detailed description of the metal's initial concentration, in addition to complementary information of oxidant and coagulant dosages are presented in Table 1.

Table 1. Experimental design proposed in the current study

Experimental design employed to assess the turbidity effect								
Turbidity (NTU)	**pH (pre-oxidation)**	**pH (coagulation - flocculation)**	**Eh (mV)**	**Arsenic (mg/L)**	**Iron (mg/L)**	**Manganese (mg/L)**	**$FeCl_3$ (mg/L)**	**NaClO (mg/L)**
1000 300 13 (control)	6.4	9.0	270	0.2	25	1.5	3.5	4.0

Experimental design employed to assess the process robustness								
Turbidity (NTU) and water sample identification	**pH (pre-oxidation)**	**pH (coagulation - flocculation)**	**Eh (mV)**	**Arsenic (mg/L)**	**Iron (mg/L)**	**Manganese (mg/L)**	**$FeCl_3$ (mg/L)**	**NaClO (mg/L)**
1000 (WS1)	6.4	8.0	270	0.015	0.13	0.48	3.5	0
1000 (WS2)				0.1	12.5	0.75		6
1000 (WS3)				0.2	25	1.5		4
1000 (WS4)				0.4	50	3		4

1.6.3 Membrane separation processes: Ultrafiltration

A commercial submerged Zeeweed ultrafiltration (UF) module by Suez Water Technologies & Solutions (filtration area: 0.047 m^2; permeability: 431.6 $L/m^2 \cdot h \cdot bar$), with a polyetherimide-based membrane and average pore diameter of 0.04 µm, was installed in a 2-L storage tank receiving the treated water leaving the sand filtration. The experiments were conducted at constant pressure (0.15 ± 0.01 bar) and temperature (25 ± 1 °C) up to a recovery rate of 50%. The ultrafiltration tank was continuously aerated (air flowrate: 0.5 Nm^3/h) as a strategy to reduce membrane fouling. After the filtration tests, a physical cleaning was performed by recirculating water for 5 minutes (2 L/min) and subsequently backwashed for 5 minutes with distilled water. In cases where the water permeability was not restored by physical cleaning, chemical cleaning was performed, consisting of an ultrasonic bath with NaOH (0.2 wt.%) and citric acid (pH=2.5) solutions for 20 min each. A schematic representation of the bench-scale set-up used for surface water treatment, including the conventional treatment process, is presented in Figure 8.

Figure 8. Schematic representation for the treatment employed for arsenic removal in conventional drinking water treatment plants.

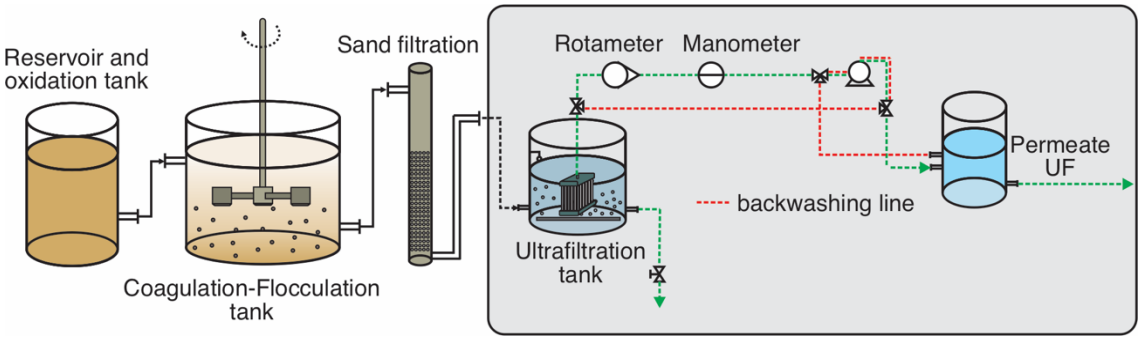

1.6.4 Statistical analysis

Microsoft Excel and OriginPro were used for statistical analysis. Although the results had a trend for a normal distribution, verified by the Shapiro-Wilk's test ($p>0.05$) and Levene's test for homogeneity, Kruskal-Wallis post-hoc with Dunn-Bonferroni tests were preferred given the number of replicates and for better confidence on the hypothesis tested. For similar reasons, Mann-Whitney U Test and Spearman were preferred for comparison between two independents groups and correlation, respectively. A confidence level of 95% was set for all statistical analyses performed.

1.6.5 Economic analysis

Capital and operating expenditures (CapEX and OpEX, respectively) were assessed under distinct perspectives. Briefly, different treatment capacities (0.108 m^3/h – 12,690 m^3/h, based on a survey made by Sorlini *et al.* [45]), in conjunction with varied membrane life span (5 – 10 years), were considered as a basis for a sensitive analysis and parametric estimating of CapEX and OpEX.

The amortization factor (AF) was calculated by annualizing the capital cost as shown in Equation 1, where i_c is the investment rate and DL the design project lifespan (15 years).

$$\mathrm{AF} = \frac{i_c \cdot (1+i_c)^{DL}}{(1+i_c)^{DL}-1} \qquad (1)$$

To calculate OpEX the variables capital cost amortization, membrane replacement, cleaning agent, chemicals, energy requirement, and maintenance were considered. A

summary of the UF system description and the utility costs considered for OpEX calculation was presented in Table 2 and

Table 3. Whenever necessary, the equipment costs were updated considering the chemical engineering cost index (CEPCI index) for 2020 and the respective index of the year in which the equipment cost was obtained.

Table 2. Variables considered for UF system design. [a][74], [b][75], [c][76], [d][77].

UF system description	
Surface water flow rate (m^3/h)	0.108 – 12,690
UF permeate flux (L/m^2.h; defined empirically)	53.1
Operating pressure (bar; defined empirically)	0.15
Recovery rate (%; defined empirically)	50
Membrane cleaning per week (defined empirically)	4
Cleaning agents (defined empirically)	NaOH and Citric acid
Pump efficiency[a]	0.75
Membrane lifespan (year)[b]	5-10
UF plant lifespan (year)[b]	15
Minimum attractive rate of return (%; defined by the authors)	15
Interest rate (% per year)[c]	6
Treated water selling costs (US$/$m^3$)[d]	0.96

Table 3. Utility costs. Currency considered whenever necessary: US$ 1.00 = R$ 5.00. Prices based on the latest Chemical Market Report made available by the Independent Commodity Intelligence Service (I.C.I.S.). [a][78]

Utility cost	
NaOH (US$/kg)	0.12
Citric acid (US$/kg)	0.65
Energy costs (US$/kWh)[a]	0.03
Membrane costs (US$/$m^2$; provided by a national supplier)	14
Maintenance rate (% CapEX; defined by the authors)	5

1.7 Results and discussions

1.7.1 Conventional process: turbidity effect

The low turbidity values reported in Table 4 after coagulation/flocculation, following values recommended by international environmental agencies (2 NTU [64]), show that the destabilization of colloidal particles was indeed efficient. Treating surface water

under high turbidity by conventional coagulation and flocculation would not be a major concern as long as the coagulant agent is dosed in the appropriate concentration. A Kruskal-Wallis test revealed that the residual turbidity between the group with initial turbidity of 1000 NTU and the control is different ($p<0.05$). The higher turbidity removal under higher initial turbidity could be explained by the increase in collision frequencies and efficiencies between particles during the coagulation-flocculation [79,80], although it does not necessarily imply a lower value for residual turbidity.

It can also be inferred from Table 4 that efficiency in turbidity removal did not necessarily imply efficient colour removal. Contrary to that, significantly higher residual apparent colour was found in media with lower turbidity values for the raw water, being these residual colour values closer to the threshold values established by the Brazilian guidelines for drinking water (15 uH [81]). The greater amount of suspended particles could have led to the formation of a higher number of flocs with higher surface area, which ultimately favored the adsorption phenomena and inter-particle bridge formation [80,82], culminating in lower residual colour.

Here is pointed out the first limitation related to conventional drinking water systems. The efficiency of the coagulation-flocculation process is subjected to several operation variables, among the medium pH. An appropriate pH for turbidity removal does not necessarily mean that it would also favor colour removal, which the most appropriate pH seems to be within the range of 3.7-4.2 when ferric salt is employed as a coagulant agent [83]. However, whether to choose for turbidity or colour removal is not an option as both parameters must attain the standard limits established for safe drinking water.

Table 4. Physicochemical characterization after coagulation/flocculation and sand filtration processes (average ± standard deviation; n=5. WS3: As: 0.2 mg/L, Fe: 25 mg/L and Mn: 1.5 mg/L). Letters in parentheses (a-f) show significantly different values within a specific physical-chemical parameter.

Treatment process		Turbidity (NTU)	pH	Eh (mV)	EC (µS/cm)	Apt. Colour (uH)
Coagulation-Flocculation	1000 NTU	2.06 ± 0.53 (a)	7.02 ± 0.04	383.4 ± 8.8	227.4 ± 4.0	4 ± 1 (d)
	300 NTU	1.56 ± 0.17 (b)	7.28 ± 0.23	364.7 ± 20.2	254.4 ± 7.1	5 ± 1 (d)
	Control	1.36 ± 0.27 (b)	7.32 ± 0.03	284.4 ± 8.1	234.2 ± 11.4	12 ± 3 (e)
Sand filtration	1000 NTU	0.47 ± 0.14 (c)	7.16 ± 0.05	298.8 ± 10.3	168.3 ± 1.0	4 ± 1 (f)
	300 NTU	0.53 ± 0.23 (c)	7.44 ± 0.10	292.4 ± 10.4	185.7 ± 11.9	4 ± 1 (f)
	Control	0.40 ± 0.06 (c)	6.67 ± 0.08	322.8 ± 1.1	210.5 ± 9.2	3 ± 1 (f)

Figure 9 summarizes the correlation between the removal efficiency of different parameters after coagulation-flocculation. It is noticeable the contribution of iron, and its complexes, for arsenic and manganese removal. In these cases, the Spearman's correlation coefficients were $r_{SpearmanFe\text{-}As} = 0.853$ and $r_{SpearmanFe\text{-}Mn} = 0.752$. Intended for a further overview of the initial variables' contribution for arsenic removal (R_{As}, %), a multivariate linear regression is presented in Equation 2. The model was statistically significant ($p<0.001$) and would be capable to explain 89.2% of the variations ($R^2=0.892$). Additionally, the analysis of variance presented in Table 5 reassured the reliability of the model obtained.

Table 5. Analysis of variance for the multivariable linear regression.

		DF	Sum of Squares	Mean Square	F Value	Prob>F
Arsenic Removal (%)	Model	7	2632.388	438.731	29.069	<0.001
	Error	56	316.942	15.092		
	Total	63	2949.331			
Manganese Removal (%)	Model	7	7544.971	1077.853	49.636	<0.001
	Error	56	1216.035	21.7149		
	Total	63	8761.007			
Iron Removal (%)	Model	7	143.554	23.925	67.326	<0.001
	Error	56	20.966	0.355		
	Total	63	164.521			

Once again, the initial concentration of iron ($C_{Fe,0}$, mg/L) would have a synergistic effect for arsenic removal, whereas high concentrations of arsenic and manganese would be

the main contributors to the lower efficiency. Other parameters such as apparent colour and turbidity would have minor effects; pH and Eh were considered non-significant terms. A multilinear regression model was also proposed for iron (R_{Fe}, %, Equation 3) and manganese (R_{Mn}, %, Equation 4) removal. Likewise, both model were significant ($p<0.001$) and capable to explain 87.2% and 86.1% of the total variations ($R^2_{Fe}=0.872$ and $R^2_{Mn}=0.861$), respectively. Their reliability was also assured after an analysis of variance (Table 5). As for arsenic, apparent colour and turbidity had minor effects in terms of iron and manganese removal, whereas iron would have a positive contribution in both cases. Once again, pH was considered a non-significant term for iron and manganese removal. The results did not necessarily suggest that pH and Eh had no contribution for the removal of these two components but, since the medium pH and Eh were kept constant in all coagulation-flocculation experiments, its contribution could not be properly assessed.

Figure 9. (a) Correlation matrix between turbidity (Turb.), electrical conductivity (EC), apparent colour (Ap. C), iron concentration, manganese concentration, and removal of arsenic after coagulation-flocculation. It is reported only the Spearman's coefficient considered significant at the level of 0.05.

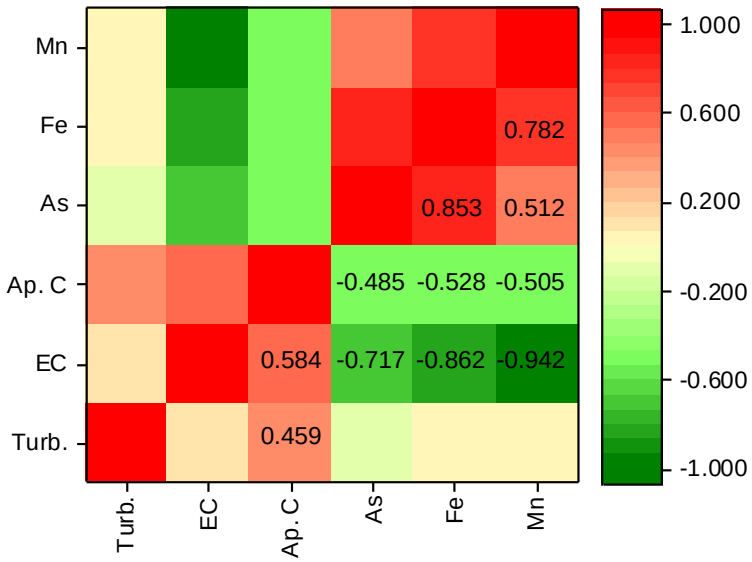

$$R_{As}(\%) = 90.55 - 0.01Turbidity(NTU) - 0.15EC\left(\frac{\mu S}{cm}\right) + 0.01App.C\ (uH) - 36.76C_{As,0}(\frac{mg}{L}) + 3.99C_{Fe,0}(\frac{mg}{L}) - 18.73.46C_{Mn,0}(\frac{mg}{L}) \quad (2)$$

$$R_{Fe}(\%) = 94.72 - 0.01Turbidity(NTU) - 0.01EC\left(\frac{\mu S}{cm}\right) - 0.01App.C\ (uH) - 15.74C_{As,0}\left(\frac{mg}{L}\right) + 0.35C_{Fe,0}\left(\frac{mg}{L}\right) - 3.82C_{Mn,0}(\frac{mg}{L}) \quad (3)$$

$$R_{Mn}(\%) = -174.12 + 0.01Turbidity(NTU) - 0.27EC\left(\frac{\mu S}{cm}\right) - 0.01App.C\ (uH) - 22.71C_{As,0}\left(\frac{mg}{L}\right) + 2.03C_{Fe,0}\left(\frac{mg}{L}\right) + 23.92C_{Mn,0}\left(\frac{mg}{L}\right) \quad (4)$$

The filtration units, designed for further pollutants removal, performed well and assured turbidity and apparent colour average values lower than 0.53 NTU and 4 uH, respectively (Table 4), without significant differences between the groups (different initial turbidity). Still, values higher than the national (0.5 NTU [81]) and international (0.3 NTU [69]) target for drinking water were still observed between the replicates.

Compared to pH and colour, higher variability was noticed for residual metals concentration when different values of initial turbidity were considered Figure 10, differing significantly from each other after coagulation-flocculation and sand filtration ($p<0.05$).

Figure 10. Residual arsenic, iron, and manganese concentration after (a) conventional coagulation and (b) sand filtration processes (average ± standard deviation; n=5, As=0.2 mg/L, Fe=25 mg/L and Mn=1.5 mg/L). *represents a residual concentration that exceeded the threshold value established by the WHO. y-axes were represented in log-scale.

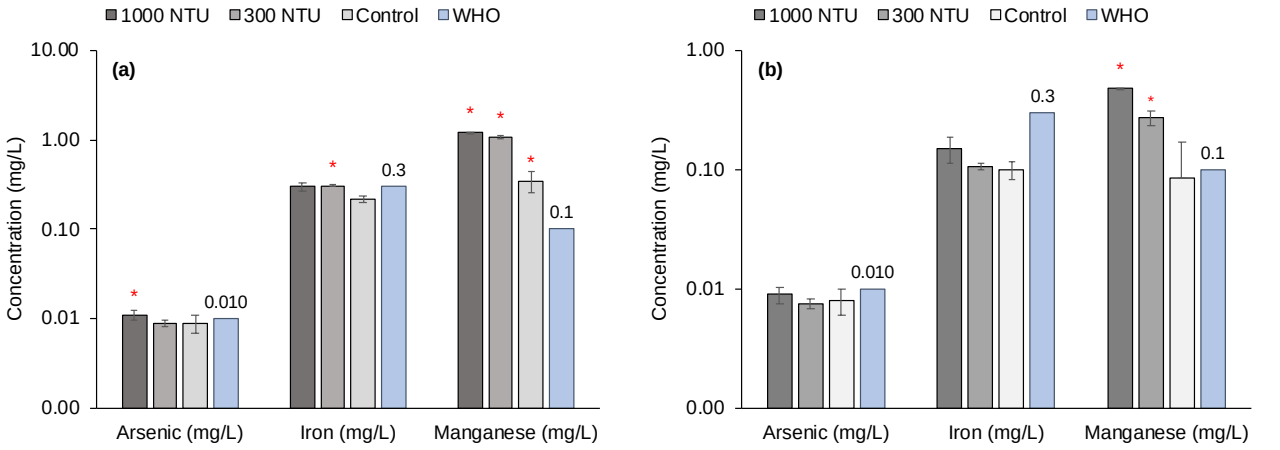

This is a point of major concern due to the impact on human health related to the prolonged consumption of contaminated water. At higher turbidities, residual concentrations had also higher median values after sand filtration, especially when the experiments with initial turbidity of 1000 NTU were compared to control experiments (Figure 11). For arsenic, 38% of the samples had concentration values greater than recommended (10 µg/L), whereas all samples attained the threshold values for iron (0.3 mg/L). Special attention should be given to the limitation of the conventional treatment process in attaining the recommended values for manganese, in which all

samples presented concentration values greater than 0.1 mg/L. The overall results demonstrated that the efficiency of attaining the standard limits for colour, arsenic, and manganese would be highly subjected to surface water turbidity.

Figure 11. Comparison between 1000 NTU and control water samples in terms of residual arsenic, iron, and manganese concentration after sand filtration (n=24. WS3: As: 0.2 mg/L, Fe: 25 mg/L, and Mn: 1.5 mg/L).

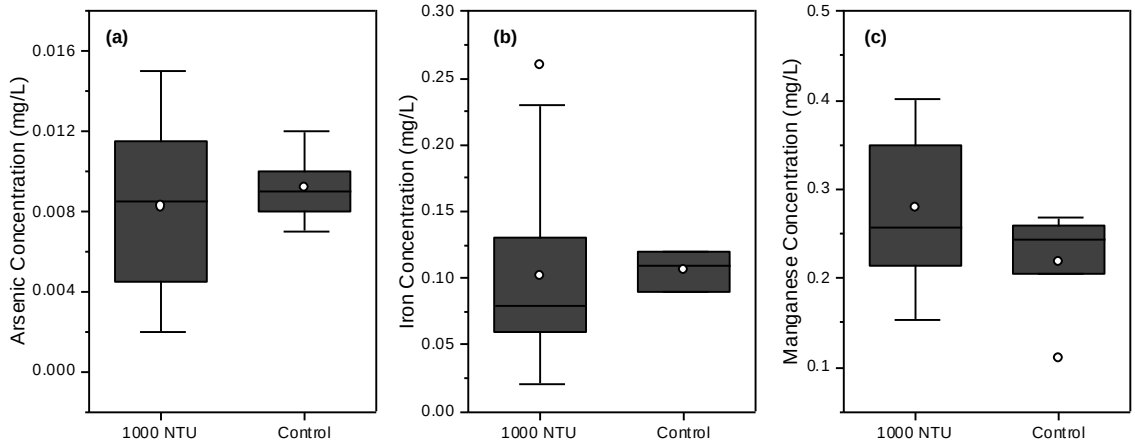

There are a few mechanisms involved in trace metals removal by conventional drinking water facilities that explain the results presented so far. In addition to favoring an appropriate formation of flocs through the destabilized colloidal particles, the higher concentrations of $FeCl_3$ would also lead to the formation of amorphous metal hydroxide flocs, in which arsenic, manganese, and iron would be entrapped and therefore removed [41]. That explains the positive correlation previously presented and seems to be a predominant mechanism for arsenic removal, complemented by the formation of insoluble precipitates as ferric arsenate ($AsFeO_4$) in case of high arsenic(V) and iron concentrations (Fe:As = 8) and if the solubility product is exceeded (<1 mg/L); for a wide pH range (3-8) [65,84]. In theory, the concomitant occurrence of both compounds would, therefore, favor their removal by conventional drinking water facilities. However, that is not a guarantee that full-scale facilities would be capable to achieve the strict limits for total arsenic in drinking water [45], most to the fact that the removal of arsenic(III) is less favored in conventional coagulation-flocculation processes [65]. Moreover, the removal of arsenic(III) is likely to be more affected by surface water quality compared to the removal of arsenic(V) [85]. Based on that, the capability of drinking water facilities in attaining arsenic removal would depend mainly on arsenic(III) concentration.

Here is highlighted the great contribution of a pre-oxidation process aiming especially for converting arsenic(III) into arsenic(V), which is not often employed in drinking water facilities even though it favors a higher removal efficiency [65].

Manganese ions, however, exceeded drinking water limits even after sand filtration (Figure 11c and Figure 10b). The median values for residual concentration significantly differ from each other (χ^2=12.500; p<0.001) and turbidity seems to have a higher interference on manganese removal. Higher values of colour reported in Table 4 after sand filtration could also be attributed to the presence of soluble species of manganese. In addition, the ion is considered more stable in its reduced and soluble form (Mn^{2+}) compared to Mn^{3+} and Mn^{4+}, and for that reason, it is more difficult to be oxidized and later removed in conventional drinking water facilities [31]. When the oxidation occurs, the complexes formed (mainly manganese dioxide) are extremely small and of poor sedimentability, not retained by sand filtration [31]. Because of that, the removal observed would have a major contribution of adsorption and entrapment process by the iron hydroxide complexes and flocs formed under high turbidity conditions [31].

These results reinforce the limitation of conventional drinking water treatment plants for trace metals removal under different surface water quality. The high variability and residual concentration values reported in Figure 11 and Figure 10 could be circumvented by stoichiometric dosages of the oxidant [48,86]. However, although effective, it can result in an unaffordable operation, due to the high costs associated with the online monitoring of the feed water quality and the increased expenditure with chemicals. This would justify the use of alternative technologies such as UF, which would be capable of retaining particles with a size greater than 0.01 µm. Thus, the colloidal particles containing arsenic and manganese formed due to the presence of iron would be rejected by the UF whereas the dissolved fraction could be precipitated even with a reduced oxidant dosage. Combining both strategies seems to be beneficial to the removal of arsenic and manganese from the surface water.

1.7.2 Conventional process: concentration effect

The robustness of conventional treatment processes was also verified under different initial concentrations of these ions. Attaining the recommended threshold for drinking

water also becomes an issue when different concentrations of metals and metalloids were considered.

The residual concentration was statistically different between the different water samples ($p<0.05$), and the process efficiency seems to be subjected to the initial concentration of the trace metals and metalloid (Figure 13). After coagulation-flocculation, the concentration of arsenic was higher than recommended in all samples excepted for water sample 1 (WS1; As 0.015 mg/L; Fe 0.13 mg/L; Mn 0.48 mg/L), although they attained the drinking water standards after sand filtration.

When it comes to manganese, its residual concentration values exceed the threshold in all water samples after coagulation-flocculation and even sand-filtration for reasons previously discussed (higher stability in its reduced and soluble form, Mn^{2+}, and the size of the complexes formed during oxidation and coagulation-flocculation). Additionally, in sand filtration and multicomponent systems, likewise in the current work and real applications, the species of iron are preferably removed compared to manganese and arsenic, leaving the active sites in the sand filter saturated and unavailable for the manganese uptake [41].

In the hypothesis that the sand filters would be saturated, increasing the oxidant dosage would not necessarily imply higher efficiency for manganese removal. In fact, the oxidant dosage used already allowed for a predominance of the colloidal fraction of arsenic and manganese after sand filtration, regardless of the turbidity and concentrations conditions Figure 12. For this reason, a stoichiometric dosage of the oxidizing agent may not be advantageous given the higher chemicals expenditure for a low contribution to the additional colloid’s formation.

Figure 12. Dissolved and colloidal fractions after sand filtration in conventional water treatment. (WS1: As: 0.015 mg/L, Fe: 0.13 mg/L and Mn: 0.48 mg/L; WS2: As: 0.1 mg/L, Fe: 12.5 mg/L and Mn: 0.75 mg/L; WS3: As: 0.2 mg/L, Fe: 25 mg/L and Mn: 1.5 mg/L; WS4: As: 0.4 mg/L, Fe: 50 mg/L and Mn: 3 mg/L)

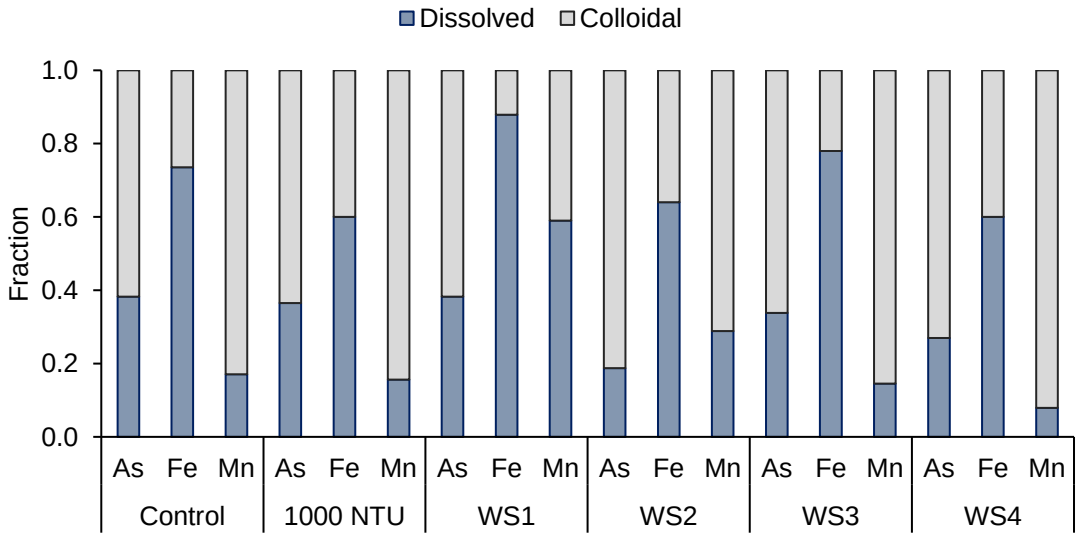

Figure 13. Comparison of residual concentration for different water samples (WS1-WS4): (a) after coagulation/flocculation and (b) after sand filtration. *represents a residual concentration that exceeded the threshold value established by the WHO. Note: y-axis is represented in log-scale. (WS1: As: 0.015 mg/L, Fe: 0.13 mg/L and Mn: 0.48 mg/L; WS2: As: 0.1 mg/L, Fe: 12.5 mg/L and Mn: 0.75 mg/L; WS3: As: 0.2 mg/L, Fe: 25 mg/L and Mn: 1.5 mg/L; WS4: As: 0.4 mg/L, Fe: 50 mg/L and Mn: 3 mg/L)

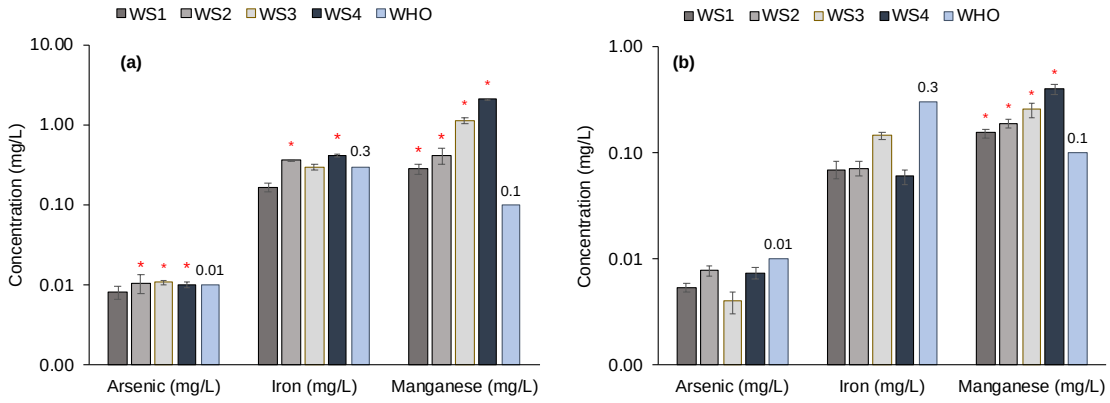

The samples obtained after coagulation-flocculation and sand filters were filtered through 0.45, 0.22, and 0.04 µm syringe filters to assess the residual concentration of these ions (Figure 14a), which did not significantly change between 0.45 and 0.22 µm syringe filters, but were significantly lower ($p=0.018$) after filtered by a 0.04 µm syringe filter. The results serve as additional evidence for two facts, the first is the predominance of colloids with radii lower than 0.45 and 0.22 µm filters pores, but higher than 0.04 µm, and the second that sand filters, which commonly present an equivalent

diameter of 10 – 100 µm [87,88], would indeed not be able to retain the colloids formed. However, the integration of sand-filters and UF membranes should allow for a significantly higher rejection of these ions due to its pore size (0.04 µm).

Figure 14. (a) Ions rejection by 0.45, 0.22, and 0.04 µm syringe filters and (b) the correlation between iron content in the feed and the residual manganese. Note: y-axis in Figure 7a was presented in log-scale.

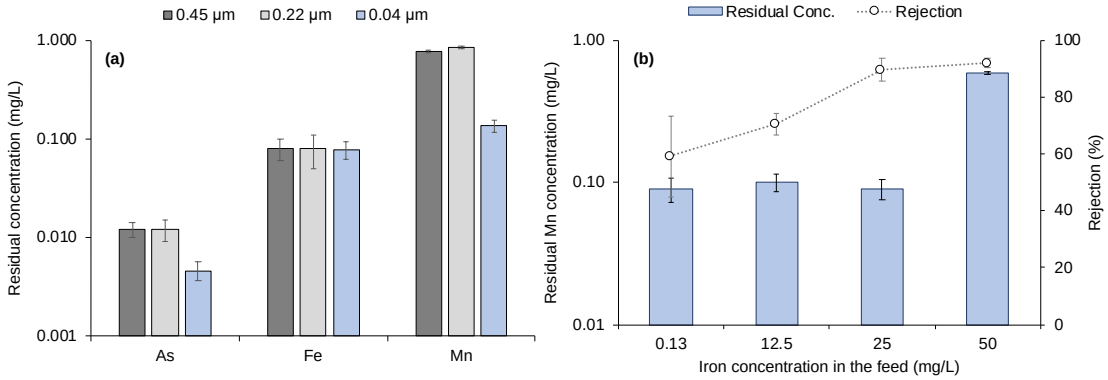

1.7.3 Conventional Treatment Process followed by Ultrafiltration

The UF performance in terms of colour and turbidity removal can be seen in Table 6. The process was robust enough that residual colour and turbidity were not significantly different when the control was compared with the 1000 NTU ($Z_{Control}$ = -0.63, p = 0.52; $Z_{1000NTU}$ = -1.10, p = 0.27) and when the different water samples (WS1-WS4, χ^2 = 7.12 p = 0.06; χ^2 = 3.58 p = 0.06 for colour and turbidity respectively) are considered. This shows that UF, when integrated with conventional treatment, can increase the quality of the water being produced and ensure national (0.5 NTU, 5 uH [81]) and international (0.3 NTU [69]) targets for turbidity and colour in drinking water.

The performance towards metal ions removal is shown in Figure 15a. It can be seen that there is no significant difference for the removal efficiency of As (Z=0.21, p=0.83) and Fe (Z=-0.94, p=0.34) by UF, regardless of the initial turbidity (13 NTU - control *vs* 1000 NTU - WS4), neither for their respective residual concentrations at different water qualities (WS1-WS4; As: χ^2=5.37 p=0.14; Fe: χ^2=4.94, p=0.17). It is also worth noting that the residual concentration of these ions complies with national and international legislation for all samples (n=5), a result not observed after sand filtration in which 38% of the samples remained above the value of 10 µg/L for arsenic.

Table 6. Physicochemical characterization after UF (average ± standard deviation; n=5). Feed water quality: WS1: As: 0.015 mg/L, Fe: 0.13 mg/L and Mn: 0.48 mg/L; WS2: As: 0.1 mg/L, Fe: 12.5 mg/L and Mn: 0.75 mg/L; WS3: As: 0.2 mg/L, Fe: 25.0 mg/L and Mn: 1.5 mg/L; WS4: As: 0.4 mg/L, Fe: 50.0 mg/L and Mn: 3.0 mg/L.

Sample		***Turbidity (NTU)***	***pH***	***Eh (mV)***	***EC (µS/cm)***	***Apt. Colour (uH)***	***As (mg/L)***	***Fe (mg/L)***	***Mn (mg/L)***
Turbidity effect	*13 NTU (Control)*	*0.28 ± 0.04*	*6.84 ± 0.05*	*288.7 ± 13.3*	*134.8 ± 6.1*	*1 ± 1*	*0.003 ± 0.002*	*0.08 ± 0.02*	*0.08 ± 0.02*
	1000 NTU (WS4)	*0.27 ± 0.03*	*7.06 ± 0.03*	*297.7 ± 5.8*	*267.4 ± 10.4*	*1 ± 1*	*0.003 ± 0.002*	*0.08 ± 0.01*	*0.13 ± 0.02*
Concentration effect (1000 NTU)	*WS1*	*0.21 ± 0.04*	*6.93 ± 0.04*	*307 ± 3.5*	*97.8 ± 5.0*	*1 ± 1*	*0.003 ± 0.002*	*0.06 ± 0.01*	*0.09 ± 0.01*
	WS2	*0.23 ± 0.03*	*7.15 ± 0.01*	*269.8 ± 6.9*	*172.5 ± 7.2*	*1 ± 1*	*0.002 ± 0.001*	*0.06 ± 0.01*	*0.10 ± 0.01*
	WS3	*0.30 ± 0.05*	*7.11 ± 0.03*	*303.1 ± 7.5*	*205.3 ± 10.9*	*2 ± 1*	*0.005 ± 0.003*	*0.08 ± 0.02*	*0.09 ± 0.01*
	WS4	*0.27 ± 0.03*	*7.06 ± 0.03*	*297.7 ± 5.8*	*267.4 ± 10.4*	*1 ± 1*	*0.003 ± 0.002*	*0.08 ± 0.01*	*0.13 ± 0.02*

Although the removal efficiency of manganese did not significantly change for an increase in water turbidity (control *vs* 1000 NTU), significant changes in removal efficiency were found for different water quality (WS1-WS2, χ^2=17.85, p<0.001). When the iron concentration increases in the samples WS1 up to WS4, the formation of insoluble complexes of manganese may be favored. This hypothesis could be visualized in Figure 14b, in which higher concentrations of iron initially available in the water leads to greater efficiencies in manganese removal through the possible formation of insoluble complexes after pre-oxidation, co-precipitation into a growing hydroxide phase via inclusion, occlusion, or surface adsorption.

Choo *et al.* [89] showed that when dosing 3 mg/L as Cl_2 the removal of iron and manganese increased upwards of 80% by the UF membrane. Similar behavior was reported by Du *et al.* [90] who showed that increasing the iron concentration up to 45 mg/L lead to an increase in antimony(III) removal by CF–UF, from ~10% to 99%. The authors also pinpointed this increase to iron co-precipitation and the formation of complexes with iron. These results reassure that UF can act on the particulate and colloidal fraction (including the dissolved fraction converted into colloidal thru pre-oxidation), which allowed for a safe drinking water supply.

Although the oxidant dosage was not sufficient to achieve potability standards by the conventional processes, it favored the formation of colloids and complexes in proportions that they were removed by the UF membrane in all water samples with the exception of WS4, in which the manganese values remained higher than recommended.

The UF performance was also be assessed in terms of permeate flux and operation stability. The difference between the permeate flux was not significant when control and 1000 NTU experiments were compared (Z = -0.626, p=0.530), neither was the initial and final permeate flux in the same experimental condition ($Z_{Control}$ = 1.148, p=0.250; $Z_{1000NTU}$ <0.001, p>0.999), which suggests that flux decay would not be a major concern under the appropriate experimental conditions.

For these experiments, the average permeate flux corresponded to 53.1 ± 1.5 L/m².h, in control, and 64.8 ± 4.8 L/m².h, in 1000 NTU (Figure 15b). Similar behavior was observed when the flux for different water samples was compared (WS1-WS4,

χ^2=3.820, p=0.281), in which no significant difference was noticed. The residual turbidity that could have had great potential for membrane fouling and permeate flux decay, was mainly removed by sand filtration. Due to that fact, phenomena as pore constriction by species that would become adsorbed within the membrane pores, pore-blocking at the membrane surface, and a cake layer formation by species rejected by the membrane were mitigated.

Figure 15. (a) Comparison between the UF removal efficiency at different turbidities (control – 1000 NTU) and water samples (WS1-WS4), (b) UF permeate flux and conductivity (n=5). (WS1: As: 0.015 mg/L, Fe: 0.13 mg/L and Mn: 0.48 mg/L; WS2: As: 0.1 mg/L, Fe: 12.5 mg/L and Mn: 0.75 mg/L; WS3: As: 0.2 mg/L, Fe: 25 mg/L and Mn: 1.5 mg/L; WS4: As: 0.4 mg/L, Fe: 50 mg/L and Mn: 3 mg/L).

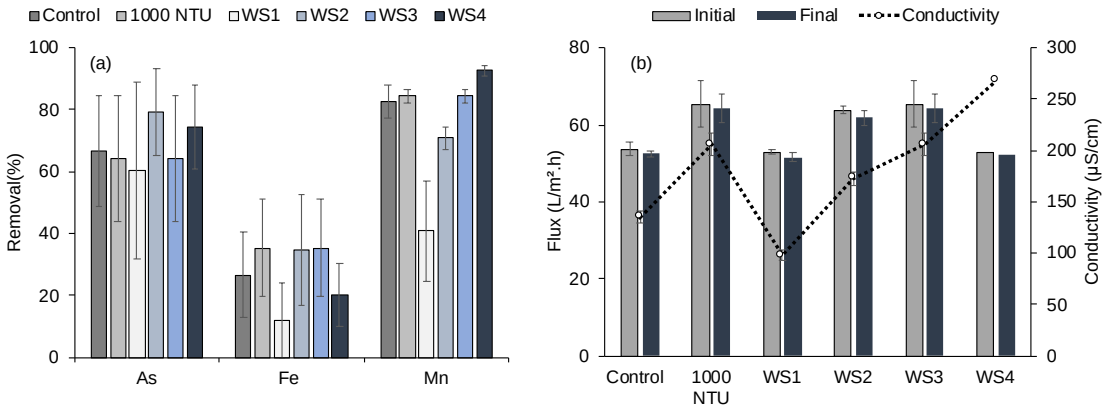

1.7.4 Economic analysis

The economic results for UF combined with the costs for conventional treatment are presented in Figure 16 (conventional treatment costs: 0.73 US$/m^3 to 0.90 US$/m^3 varying accordingly with the treatment capacity, 0.11 - 12,960 m^3/h [77]). The overall treatment costs (conventional treatment cost + ultrafiltration cost) would hover around 0.81 – 0.98 US$/m³, in which the membrane replacement was the main contributor for the OpEX values related to UF Table 7.

Table 7. Operating expenditures breakdown for a treatment capacity: 12,690 m³/h and membrane lifespan of 7 years.

OpEX variable	Value
Membrane replacement (US$/year)	**2,483,716.71**
Chemicals (US$/year)	19,190.34
Energy costs (US$/year)	40,019.18
Maintenance (US$/year)	1,952,307.69
Amortization costs (US$/year)	4,020,299.92
Annual expenditures (US$/year)	8,515,533.84
OpEX (US$/m³)	0.077

Due to that fact, membranes with a longer lifespan contributed to a lower OpEX as shown in Figure 16a, varying from 0.07 – 0.08 US$/m³ for the UF solely. Given that the physicochemical quality of the water being treated (after the sand filters), complemented by the development of more resistant membranes, it is reasonable to assume that the membranes would have a lifespan longer than five years. That is a positive aspect that favors the process implementation especially in cases of decentralized water treatments in which the treatment capacity is reduced.

In the event of a UF being implemented in water treatment plants with different capacities, the process would become more economically attractive in facilities that have a treatment flowrate greater than 1,620 m³/h (Figure 16b) given that the OpEX values start to show little to no reduction from then on. The decrease in the CapEX per treatment capacity for the UF implementation is driven by the gains in treatment capacity while the cost increases. In all cases, the UF costs contribution to the total OpEX, which includes the conventional treatment costs, ranged from only 8.77 to 9.63%.

From a broader perspective, a higher treatment cost could be compensated by other environmental and human health gains related to a better drinking water supply in the event of higher turbidity conditions and arsenic concentration [91]. Due to that fact, health benefits should be included whenever possible as decision support in the drinking water context. Ahmad et al. [92] demonstrated that lowering As concentration to <1 µg/L in the Netherlands could result in an annual benefit of 8.4–16.3 million US$, mostly to the fact that the health care costs would be reduced.

Figure 16. Sensitive analysis considering (a) different membranes lifespan (treatment capacity of 0.108 m³/h) and (b) adduction flowrates (membrane lifespan of 7 years).

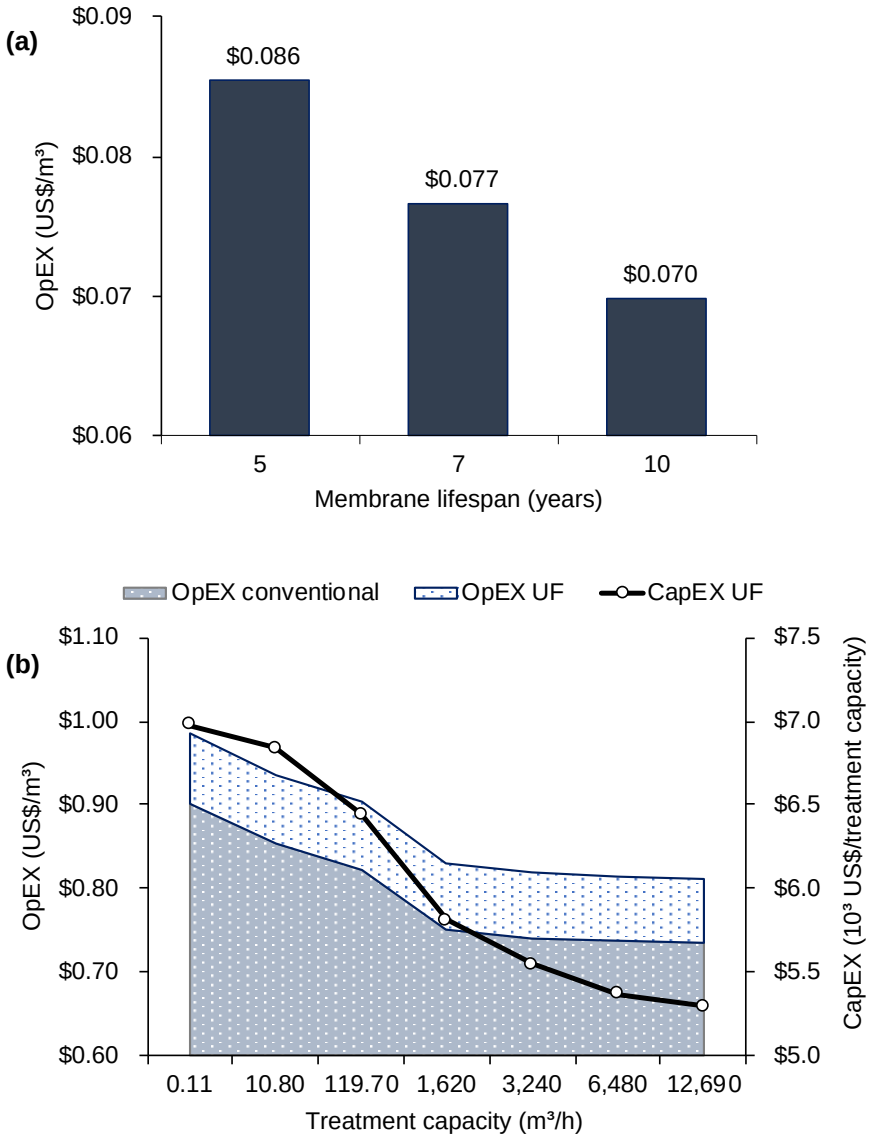

1.7.5 Critical steps and perspectives on drinking water facilities improvement

Due to the increasing water scarcity and/or quality deterioration, the population has leaned towards the use of water sources heavily contaminated with arsenic and other ions. Because of that, as pointed out by Chowdhury [93], proper strategies for water treatment and management are undergoing rapid advancement. It is expected that there will be more development in the next years than it had during the past 2000 years. For that, different routes can be employed to adequate water resources into the standards required for human consumption, each with its advantages and disadvantages.

Besides that, the removal of As(III) in conventional DWTPs is highly subjected to the physical-chemical characteristics and the composition of the surface water [85], with a pronounced reduction in the efficiency of the process in cases of higher concentration of electrolytes and natural organic matter. Nonetheless, there is a consensus in the literature that removing As(III) from water is laborious, and requires special attention due to its impacts on the environment and human health [85].

From the previous sections it could be seen that the conventional drinking water treatment process alone did not achieve national and international standards for drinking water, however, the integration with UF showed an increase in overall performance in ions retention and low flux decline. Although it seems that the UF contribution for the overall ion retention efficiency in the process is low (Figure 17), the UF proved to be of great importance for meeting the drinking standards. In this sense, UF can be used to retrofit DWTP due to the increase in the concentration of ions such as arsenic in surface water.

Figure 17. Contribution of each step for the removal of ions. Removal was calculated considering the feed and the residual concentration of each step (global removal).

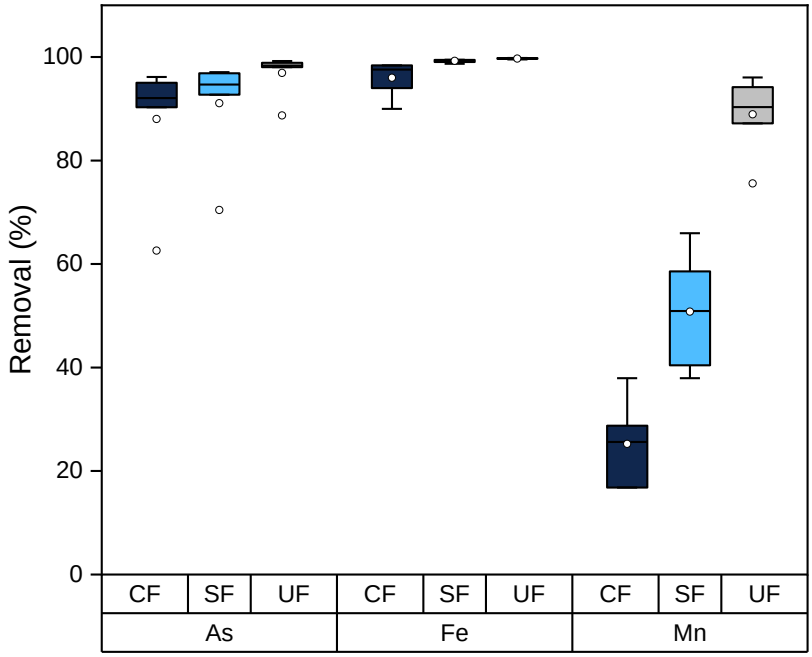

As demonstrated in the economic analysis, the implementation of UF systems in DWTPs with low treatment capacity is not advantageous due to the high OpEX. However, this scenario can, and has been changing over the years due to several factors such as (i) the development of new technologies and polymeric materials for the manufacture of membranes; (ii) the implementation of stricter legislation for drinking water quality and (iii) the increase in contamination by arsenic in surface and groundwater. All these aspects contribute to the transformation of previously infeasible (from an economic point of view) projects into an indispensable necessity.

CHAPTER 3

RECYCLED REVERSE OSMOSIS MEMBRANE FOR ARSENIC REMOVAL FROM HIGH TURBIDITY WATERS: RETROFITTING CONVENTIONAL DRINKING WATER TREATMENT PROCESS

MOREIRA, Victor Rezende et al. Recycled reverse osmosis membrane combined with pre oxidation for improved arsenic removal from high turbidity waters and retrofit of conventional drinking water treatment process. **Journal of Cleaner Production**, p. 127859, 2021. DOI: 10.1016/J.JCLEPRO.2021.127859

1.8 Introduction

The spread scenario of surface and groundwater contaminated by arsenic points out the necessity for innovative, decentralized, and low-cost treatment processes. One alternative previously presented in Chapter 2 is the implementation of pre-oxidation and dead-end ultrafiltration processes in conventional drinking water facilities. The strategy effectively converted soluble species into complexes and colloids that were partially removed by coagulation-flocculation and sand filtration [94]. Dead-end ultrafiltration served as an additional barrier to their elimination, with a few exceptions of manganese complexes. It was also evidenced that an effective pre-oxidation required a constant adjustment of the oxidant dosage, a procedure not often employed in drinking water facilities.

A different strategy is presented in Chapter 3, which relies on the use of different ultrafiltration (UF) membranes right after the pre-oxidation in replacement of the conventional processes (coagulation-flocculation and sand filtration). Besides iron and manganese, aluminum was introduced as a third-party interferer for arsenic removal. The hypothesis previously presented remained. Given the size of UF membranes pores (0.01 µm) and the size of the complex and colloids formed after a pre-oxidation (0.01 – 0.2 µm [46,56,57]), it can be expected a higher removal efficiency of arsenic, iron, manganese, and aluminum by UF compared to conventional sand filtration (which has an average equivalent diameter of 10-100 µm [87,88]).

Currently, there are two primary types of UF modules are submerged (UFs) and pressurized (UFp), differing mainly from their operation mode, but also permeate flux, fouling propensity, and costs related to their acquisition and operation [59]. UFs has been widely used for water and wastewater treatment due to their lower energy consumption [60] compared to UFp and other membrane separation processes. UFp, in its turn, has generally higher permeate flux [59,60], a favorable aspect that should be taken into account while deciding for the most cost-effective alternative. Still, these are modules that could present a membrane cost of 980 US$ per unit (equivalent to 25.13 US$/$m^2$), which summed up to their cost for annual replacement could represent an investment of 1,176 US$ [61]. Based on that, de Paula & Amaral [61] proposed the conversion of end-of-life reverse osmosis (RO) membrane into ultrafiltration-like membranes by means of its chemical oxidation. The worldwide amount of RO

membranes annually disposed in landfills reached 16,500 tons (equivalent to 37,125 m^3) in 2018 [95], clearly demonstrating the magnitude of the imminent elimination challenge to be projected for the next decade. Rather than their disposal, end-of-life RO could be recycled by a low-cost oxidative treatment producing a porous membrane with properties similar to ultrafiltration (UF) membranes [96]. According to the authors, the recycled RO membrane (UFr) would present a membrane cost of 8.53 US$ per unit (equivalent to 0.22 US$/$m^2$), besides the environmental gains related to the reuse of a spent membrane.

For being an affordable technology, the use of UFr membranes would meet a first pre-requisite for novel technologies being sought for a safe drinking water supply [97]. The outcome could be a reliable water service in terms of quantity and/or quality and an alternative to the improvement of existing centralized drinking water facilities, often prohibitively costly and time-consuming [98]. Extending the use of UFr, therefore, could reduce the gap between the water demand and its supply observed over the past decades, as a decentralized drinking water technology. Their effectiveness for surface water treatment in terms of water permeability and salinity rejection has been previously assessed by de Paula et al. [62], and their use for arsenic, iron, manages and aluminum removal seems to be a promising alternative.

The current Chapter compares the efficiency of a UFr with commercials UFs and UFp for contaminated surface water treatment, permeate flux and fouling propensity, as strategies for a safe drinking water supply. A pre-oxidation stage was considered prior to the filtration experiments. The treatment trail proposed (pre-oxidation followed by UF units) was also compared with the conventional treatment processes. Surface water of different turbidities was simulated considering that surface water quality would affect the overall process efficiency in arsenic removal [54]. High-turbidity waters are commonly observed along rainy seasons, representing a challenge for water treatment facilities and implications for a safe-drinking water supply [69]. Although turbidity does not necessarily imply a direct risk to public health, the suspended solids responsible for turbidity can serve as a carrier to arsenic, metal ions, and microbial pathogens in surface water samples [69,70]. The decision for the most appropriate strategy also considered besides the performance aspects their economic feasibility, comparing the payback period, net present value (NPV), rate of return (RoR) in addition to their capital

(CapEX) and operating (OpEX) expenditures, for the three alternatives investigated (UFs, UFp, and UFr).

1.9 Material and methods

1.9.1 Chemicals and reagents

Stock solutions (1.0 and 10 mg/L) of arsenic, iron, manganese, and aluminum were prepared with $Na_2HAsO_4.7H_2O$, $FeCl_3$, $MnSO_4.H_2O$, and $Al_2(SO_4)_3$, respectively, purchased by NEON® and used without further purification. Sulfuric acid and sodium hydroxide solutions (0.01 mol/L; pH=2 and 12, respectively) were used to adjust the medium pH whenever necessary. Sodium hypochlorite (NaClO, 6% aqueous solution) employed as an oxidant agent was supplied by Fisher Chemical™.

1.9.2 Water sampling and physicochemical characterization

A description for surface water and sediments samples were previously presented in Section 1.6.1. Additionally to arsenic, iron and manganese, aluminum was spiked in concentrations ranging 0.09 – 1 mg/L which values were defined based on monitoring studies. Similar procedure was employed for samples preservation and characterization. As for arsenic, iron, and manganese, aluminum concentration values were also determined by inductively coupled plasma mass spectrometry (ICP-MS; method 3125B; lower quantification limits: 0.001 mg/L).

1.9.3 Recycled reverse osmosis membrane

The recycling procedure followed the recommendations proposed by de Paula et al. [62] for higher effectiveness in terms of RO membrane conversion. The procedure consisted of the immersion of a full end-of-life thin-composite RO membrane module (39 m^2), without its dismantling, in a commercial sodium hypochlorite bath (contact intensity: ~300,000 ppm.h) at room temperature (25 ^oC), for 4 h. The end-of-life spiral wound RO membrane (FilmTec BW30, average permeability 3.0 L/h.m²bar) was previously employed in a desalination plant. The UFr exhibited a permeability of 79.1 ± 5.8 L/h.m²bar, salt rejection (NaCl 2.0 g/L) of 16.7 ± 2.5%, contact angle of 75.5 ± 1.7°, and root-mean-square roughness of 6.13 ± 0.86 nm. The increased permeability and reduced saline rejection are associated with the changes in the membrane selective layer. These values are similar to those observed for UF-like membranes,

suggesting that the membrane was effectively recycled. Lastly, the membrane was cut to fit into the membrane cell holder (63.6 cm^2) where filtration tests were carried out.

1.9.4 Conventional treatment and filtration experiments

Water samples underwent a pre-oxidation procedure using NaOCl for 1 h in a Jar-test under constant agitation (120 rpm). A control group, still spiked with arsenic, iron, and manganese but without a pre-oxidation, was also evaluated for comparison purposes. Different oxidant dosages were assessed (0 – 8.0 mg/L) to define the most appropriate dosage for different surface water qualities. In these experiments, a conservative scenario was considered in terms of medium turbidity, set as 1,000 NTU. Before coagulation-flocculation, the medium pH was adjusted to 6.4 and $FeCl_3$ was used as a coagulant agent. The paddles were first operated at rapid mixing (100 rpm; 1 min), followed by 68, 44, 37, and 26 rpm all held for 4 min each. The media were left to settle for 5 min (settling velocity: 1.5 cm/s) and the supernatant was collected for physicochemical characterization and further sand filtration. A down-flow sand filtration system was used with a height of 240 mm and inner diameter of 19 mm, filled with conventional sand with an average particle diameter of 0.297 – 1.18 µm (depth: 150 mm). Before each test, the filters were compacted using deionized water (500 mL). The experimental design considered in these experiments is presented in Table 8. Previous studies (data not shown) were carried out to assess the most appropriate oxidant concentration range, coagulant dosages, in addition to coagulation/flocculation diagrams as a function of medium pH, being adopted the most adequate operating conditions.

Table 8. Experimental design proposed for defining the most appropriate oxidant dosage.

Turbidity (NTU) and water sample identification	pH (pre-oxidation)	Arsenic (mg/L)	Iron (mg/L)	Manganese (mg/L)	Aluminium (mg/L)
1000 (WS5)	6.4	0.015	0.13	0.48	0.09
1000 (WS6)		0.1	12.5	0.75	0.50
1000 (WS7)		0.4	50	3.0	1.00
1000 (WS8)		0.2	25	1.5	-

A commercial submerged Zeeweed ultrafiltration module (UFs) by Suez Water Technologies & Solutions (filtration area: 0.047 m^2; permeability: 431.6 $L/m^2 \cdot h \cdot bar$), with a polyetherimide-based membrane and average pore diameter of 0.04 μm. The pressurized UF modules (UFp) were supplied by DuPont (filtration area: 0.3 m^2, permeability: 468 $L/m^2 \cdot h \cdot bar$), with a polyetherimide-based membrane and average pore diameter of 0.04 μm. The filtration experiments were conducted at a constant pressure (UFs: 0.2 ± 0.1; UFp: 0.4 ± 0.1 and UFr: 1.0 ± 0.1 bar) and temperature (25 ± 1 °C). UFs module was continuously aerated (air flowrate: 0.5 Nm^3/h) and the UFp intermittently (air flowrate: 2.0 Nm^3/h, 30 seconds every 15 minutes) as a strategy to reduce membrane fouling. The crossflow velocity in UFr experiments (filtration area: 63.6 cm^2, permeability: 79.1 $L/m^2 \cdot h \cdot bar$) were defined as 0.198 cm/s based on previous studies [62]. After filtration, a physical cleaning was performed by recirculating deionized water for 5 minutes (2 L/min). In cases where the water permeability was not restored, chemical cleaning was performed consisting in an ultrasonic bath with NaOH (0.2 wt.%) and citric acid (pH = 2.5) solutions for 20 min each. The efficiency of the filtration experiments was assessed under different turbidities (100, 300, and 1000 NTU) by means of arsenic, iron, and manganese rejection efficiency, recovery rate, flux decline (J/J_0), and fouling propensity considering the membrane pore blocking models developed by Hermia [99]. A schematic representation of the bench-scale set-up used for surface water treatment, including the conventional treatment process, is presented in Figure 18.

Figure 18. Schematic representation of (a) conventional drinking water treatment (b) UFs, (c) UFp, and (d) UFr in a lab-scale set-up.

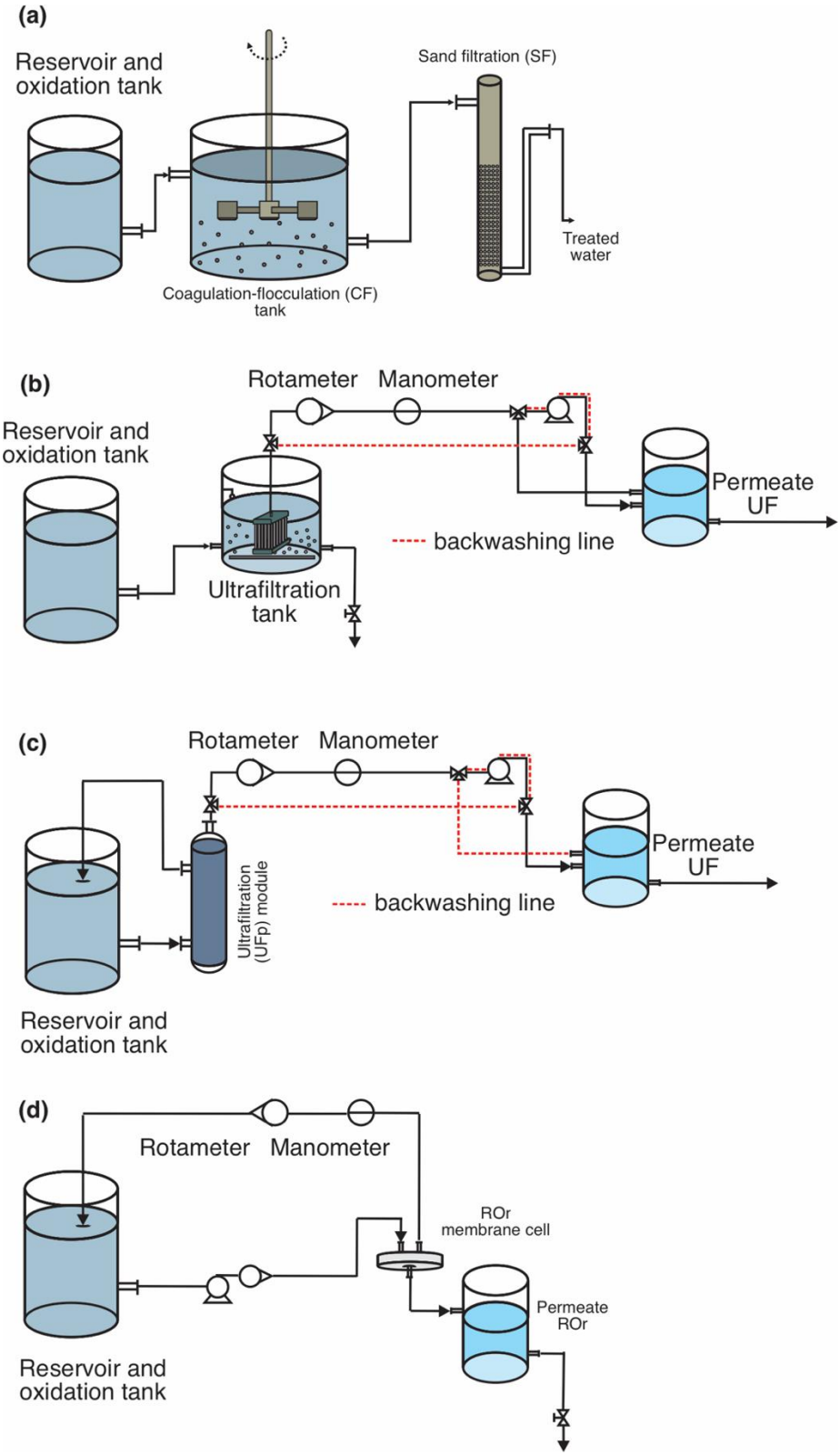

1.9.5 Preliminary economic analysis

The capital and operating expenditures (CapEX and OpEX, respectively), the net present value (NPV), and the rate of return (RoR) were assessed for different treatment perspectives and conditions. Moreover, a sensitive analysis was carried out for the feed flow rate, considering values from a survey reported by Sorlini *et al.* [45] (0.108 m³/h – 12,690 m³/h). Savings with chemicals, monitoring systems, wage labor, and routine analysis, no longer required by UFs, UFp, and UFr when replacing the conventional treatment processes, were defined as the difference between the OpEX estimated for the membrane and the conventional treatments [77]. This savings was then set as revenue and used as basis for NPV and RoR estimations.

The NPV, RoR and the payback period for the investment were calculated considering a design project lifespan (DL) of 15 years. The NPV was calculated using Equation 5, in which S is the profit or loss in the year (cash flow – considered as the difference between the cost associated with the conventional treatment and the one being proposed), i is the interest rate considered, t is the number of the year. The RoR, represented by the variable i, was calculated using Equation 6. To estimate the payback period, the capital cost was divided by the annual cumulative cash inflow.

$$NPV = \sum_{t=1}^{n} \frac{S}{(1+i)^t} \quad (5)$$

$$0 = \sum_{t=1}^{n} \frac{S}{(1+i)^t} \quad (6)$$

The amortization factor (AF) was calculated by annualizing the capital cost, as shown in Equation 7, where i_c is the investment rate.

$$\mathrm{AF} = \frac{i_c \cdot (1+i_c)^{DL}}{(1+i_c)^{DL}-1} \quad (7)$$

The OpEX was calculated considering different variables such as the capital cost amortization, membrane replacement, cleaning agent, chemicals, energy requirement, and maintenance. A summary of the system description and the utility costs considered for OpEX calculation was presented in Table 9. Whenever necessary, the equipment costs were updated considering the chemical engineering cost index (CEPCI index)

for 2020 and the respective index of the year in which the equipment cost was obtained.

Table 9. Variables considered for the design of the UF systems. Chemical prices were based on the latest Chemical Market Report made available by the Independent Commodity Intelligence Service (I.C.I.S.). [a][74], [b][75], [c][76], [d][100], [e][78]

Description	UFs	UFp	UFr
Surface water flowrate (m^3/h)		0.108 – 12,690	
Permeate flux (L/m^2.h; defined empirically)	101.8	63.0	53.3
Operating pressure (bar; defined empirically)	0.2	0.4	1.0
Recovery rate (%; defined empirically)		80	
Membrane cleaning per week (defined empirically)		4	
Cleaning agents (defined empirically)		NaOH and Citric acid	
Pump efficiency[a]		0.75	
Membrane lifespan (year)[b]	7	5	2
UF plant lifespan (year)[b]		15	
Minimum attractive rate of return (%; defined by the authors)		15	
Interest rate (% per year)[c]		6	
Concentrate disposal costs (US$/$m^3$)[d]		1.3	
Oxidant dosage (mg/L; defined empirically)		4.0	
Utility cost			
NaOH (US$/kg)		0.12	
Citric acid (US$/kg)		0.65	
NaClO (US$/kg)		0.50	
Energy costs (US$/kWh)[e]		0.03	
Membrane costs (US$/$m^2$; provided by a national supplier)		14	
Maintenance rate (%CapEX; defined by the authors)		5	

1.9.6 Statistical analysis

OriginPro and Statistica 12 were used for statistical analysis. Kruskal-Wallis post-hoc with Dunn-Bonferroni, Mann-Whitney U Test, and Spearman correlation tests were preferred given the number of replicates and for better confidence on the hypothesis tested. A confidence level of 95% was set for all statistical analyses performed.

1.10 Results and discussions

1.10.1 Conventional drinking water treatment

Substances as sulfide, total organic carbon, and metal ions are recurrent compounds in surface water and interfere in the oxidant demand, which requires a constant

adjustment throughout a conventional drinking water facility operation [101]. Due to that fact, surface water with different pollutants concentrations was used to assess the most adequate oxidant, which the results for residual concentration after pre-oxidation, followed by coagulation-flocculation, are shown in Figure 19.

Figure 19. Residual concentration of aluminum, arsenic, iron and manganese for different water qualities after coagulation-flocculation (n=5). (a) WS5 (Al 0.09 mg/L; As 0.015 mg/L; Fe 0.13 mg/L; Mn 0.48 mg/L), (b) WS6 (Al 0.50 mg/L; As 0.1 mg/L; Fe 12.5 mg/L; Mn 0.75 mg/L), (c) WS7 (Al 1.0 mg/L; As 0.4 mg/L; Fe 50.0 mg/L; Mn 3.0 mg/L), (d) WS8 (As 0.2 mg/L; Fe 25.0 mg/L; Mn 1.5 mg/L).

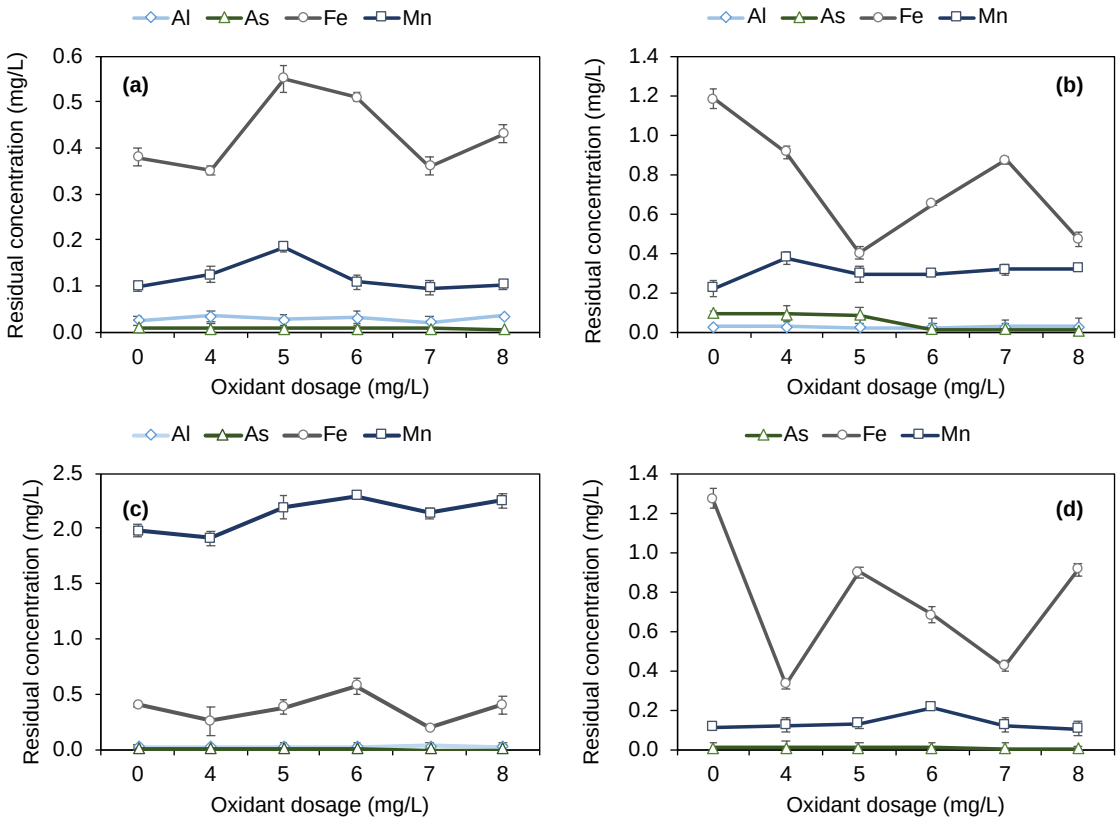

An increase in oxidant dosage not always resulted in a lower residual ion concentration. Considering the first water quality in Figure 19a (Al 0.09 mg/L; As 0.015 mg/L; Fe 0.13 mg/L; Mn 0.48 mg/L) the lowest sum of metal ions concentration after coagulation-flocculation was for the oxidant dosage of 4 mg/L; however, without a significant difference ($p = 0.328$) compared to 0 mg/L of oxidant. In this scenario, oxidant dosage could be left out of the process given the economic savings without compromising the process performance. The second water sample (Figure 19b) showed the lowest sum of ions available at the dosage of 5 mg/L, but the lowest residual arsenic concentration occurs at the dosage of 6 mg/L (a reduction from 0.089 ± 0.011 mg/L to 0.005 ± 0.002 mg/L). In that case, it would be interesting to adopt a

higher dosage of oxidant to achieve lower residual concentrations of arsenic, providing greater robustness to the process. For the last two qualities of water (WS7 – WS8), the oxidant dosage that was most effective in removing the ions was 4 mg/L.

The residual aluminum concentration remained low in all water samples (WS5-WS7), with no significant differences between different oxidant dosages and the same water sample (WS5: p=0.218; WS6: p=0.109 and WS7: p=0.445) or for a fixed oxidant dosage and different water samples (p>0.071). Given the pH and Eh conditions that the experiments were performed, which in turn are similar to those used in real drinking water treatment plants [1], the species of aluminum would be mostly in their precipitated form without even the requirement for a pre-oxidation process. The fact is further evidenced by the low Spearman coefficient obtained between the residual aluminum concentration and the oxidant dosage (r_{WS5} = 0.010; r_{WS6} = 0.106 and r_{WS7} = 0.173).

Stable colloids and precipitated species of aluminum were also observed by Hu et al. [102] for the pH value similar to that used in this study, which reinforces the results presented. These results also suggest a low contribution from the aluminum species to the oxidant requirement, a fact evidenced when comparing WS7 and WS8 that presented the same dosage (4 mg/L) even though WS8 considered the aluminum as a contaminant. Under those circumstances, aluminum was discarded from our subsequential filtration experiments presented in section 3.3.2.

A synergetic behavior could be seen in Figure 19a and Figure 19c, where a higher residual concentration of iron was followed by a higher residual concentration of manganese. Ellis et al. [103] reported similar behavior, which showed that the oxidation of manganese in the presence of iron is favored due to the possible adsorption of manganous ions onto iron oxides or the coprecipitation of iron and manganese. The Spearman correlation coefficient confirmed the hypothesis that the residual concentration of manganese was correlated with the iron residual content (r=0.637; p=0.034 for Figure 19c). The other water qualities do not exhibit this correlation, probably because the initial iron concentration was not enough to show any significant effect on manganese residual concentration. The experiments performed with the most appropriate oxidant dosage were selected for filtration through the sand filters and the results are shown below in Table 10.

Table 10. Water physical-chemical characterization for the effect of oxidant dosage and sand filtration. C/F: coagulation-flocculation (average ± standard deviation; n=5). *Sand filtration followed coagulation-flocculation preceded by oxidation with NaClO.

	NaClO (mg/L)	Turbidity (NTU)	pH	Conductivity (µS/cm)	Colour (uH)	Al (mg/L)	As (mg/L)	Fe (mg/L)	Mn (mg/L)
WS5	-	1010 ± 24	6.40 ± 0.09	69.8 ± 1.5	1613 ± 27	0.081 ± 0.006	0.011 ± 0.003	0.09 ± 0.01	0.523 ± 0.027
C/F	-	4.92 ± 0.53	6.41 ± 0.11	112.2 ± 3.1	14 ± 2	0.024 ± 0.005	0.008 ± 0.002	0.38 ± 0.04	0.098 ± 0.007
C/F with oxidant	4	4.86 ± 0.42	6.63 ± 0.23	128.6 ± 6.5	14 ± 1	0.034 ± 0.009	0.007 ± 0.001	0.35 ± 0.02	0.124 ± 0.058
Sand Filtration*	-	0.26 ± 0.02	6.55 ± 0.10	92.2 ± 3.3	5 ± 1	0.014 ± 0.002	0.008 ± 0.001	0.08 ± 0.01	0.056 ± 0.006
WS6	-	1016 ± 36	6.41 ± 0.12	126.8 ± 2.8	1723 ± 21	0.436 ± 0.038	0.137 ± 0.019	9.31 ± 0.01	0.090 ± 0.003
C/F	-	4.72 ± 0.33	6.56 ± 0.09	170.7 ± 11.2	18 ± 3	0.027 ± 0.004	0.093 ± 0.001	1.18 ± 0.11	0.221 ± 0.037
C/F with oxidant	6	4.67 ± 0.47	6.51 ± 0.21	173.9 ± 9.87	12 ± 2	0.019 ± 0.002	0.011 ± 0.007	0.65 ± 0.07	0.211 ± 0.059
Sand Filtration*	-	0.12 ± 0.01	7.08 ± 0.16	124.8 ± 7.2	1 ± 1	0.018 ± 0.002	0.009 ± 0.002	0.02 ± 0.01	0.039 ± 0.008
WS7	-	993 ± 15	6.44 ± 0.04	609.2 ± 14.2	1712 ± 11	0.891 ± 0.053	0.428 ± 0.031	45.73 ± 3.29	2.732 ± 0.281
C/F	-	4.98 ± 0.39	6.49 ± 0.11	399.7 ± 21.3	12 ± 3	0.024 ± 0.002	0.009 ± 0.002	0.40 ± 0.02	1.980 ± 0.022
C/F with oxidant	4	4.91 ± 0.28	6.47 ± 0.16	370.9 ± 8.91	9 ± 2	0.023 ± 0.007	0.008 ± 0.003	0.26 ± 0.07	1.910 ± 0.007
Sand Filtration*	-	0.45 ± 0.03	7.37 ± 0.22	262.1 ± 21.3	5 ± 1	0.022 ± 0.002	0.007 ± 0.002	0.12 ± 0.04	0.104 ± 0.003
WS8	-	1022 ± 34	6.43 ± 0.07	308.1 ± 2.2	1623 ± 14	-	0.244 ± 0.017	23.87 ± 1.08	1.838 ± 0.331
C/F	-	4.62 ± 0.52	6.35 ± 0.17	236.4 ± 5.6	8 ± 2	-	0.008 ± 0.003	1.27 ± 0.08	0.111 ± 0.073
C/F with oxidant	4	4.51 ± 0.36	6.32 ± 0.15	254.3 ± 8.2	10 ± 2	-	0.009 ± 0.005	0.33 ± 0.05	0.122 ± 0.037
Sand Filtration*	-	0.19 ± 0.01	7.28 ± 0.32	283.5 ± 7.1	1 ± 1	-	0.009 ± 0.002	0.05 ± 0.02	0.059 ± 0.012

From Table 10 it is possible to note a high removal rate of color and turbidity right after coagulation-flocculation. The coagulant ($FeCl_3$) is responsible for an adjustment on the solids' surface charge, so existing particles in the surface water can agglomerate or be embedded into a flocculated precipitate. Hence, turbidity and color removal can be attributed to the adsorption onto the flocs surface or coprecipitation by inclusion/occlusion during floc formation [104,105]. These flocs are then settled and ultimately remove colour from the surface water. The sand filtration units served as an additional contribution to turbidity removal, achieving values below the recommendation by the World Health Organization for drinking water (0.3 NTU) except for WS7, whereas the threshold value for colour (4 uH, from World Health Organization) was disrespected in WS5 and WS7.

While the removal of color and turbidity was high, in some cases the conventional coagulation-flocculation and sand filtration were not enough to comply with the legislation regarding the residual concentration of arsenic and manganese. A first explanation for the removal observed would be the entrapment of arsenic, iron, and manganese by amorphous hydroxide flocs formed (iron and aluminum-based [102]) during coagulation-flocculation, which were later removed by decantation and sand filtration. That would be the main pathway for manganese removal since its reduced form (Mn^{2+}) is more stable than its oxidized species (Mn^{3+} and Mn^{4+}). Hence, colloids and insoluble complexes of manganese are hardly obtained after a pre-oxidation process and, whenever formed, they are extremely small in size and would not be retained by the sand filtration units [31]. The experimental conditions employed were also favorable to ferric arsenate ($AsFeO_4$) formation, an insoluble compound obtained when the iron:arsenic ratio is close to eight, with a solubility product below 1 mg/L [65].

In a conventional treatment process, even when preceded by a pre-oxidation, residual concentration higher than the threshold values (arsenic: 0.01 mg/L and manages: 0.1 mg/L, from World Health Organization) can occur, especially at higher concentrations of arsenic and manganese.

In Chapter 2 we discussed the alternative of dosing the oxidant at stoichiometric ratios as a strategy to overcome the limitations of metallic species and arsenic removal. However, it was demonstrated that most species are already in their colloidal form, and the increase in the oxidant dosage to convert the remaining species would be

costly. The strategy would also require the installation of systems to monitor the surface water quality and adjust the oxidant dosage. Another alternative is the implementation of a more robust process, in our case UF membranes. Under those circumstances, a higher chemical dosage will no longer be necessary as UF membranes would act as an additional physical barrier that would withstand possible fluctuations in the arsenic, iron, and manganese concentrations after pre-oxidation.

1.10.2 Comparison of recycled and commercial membranes

Figure 20 presents the residual concentration for arsenic, iron, and manganese obtained for the permeate of the UFr, UFs, and UFp. Residual arsenic concentrations in waters whose initial turbidity was 100 NTU varied between 0.101 – 0.142 mg/L without a pre-oxidation step. The values were significantly lower when the UFr permeate was compared to the UFs (Figure 20a). In the processes preceded by a pre-oxidation, the residual arsenic concentration (100 NTU: 0.001 – 0.006 mg/L; 300 NTU: 0.001 – 0.008 mg/L, and 1000 NTU: 0.001 – 0.008 mg/L) showed no significant difference between the different systems (UFs, UFp, and UFr) nor between the different conditions of initial turbidity. In these cases, the threshold values recommended by the World Health Organization were reached for the permeate of all processes (10 µg/L).

The contribution of a pre-oxidation process is evident for iron removal (Figure 20b) at levels that met the values recommended by the World Health Organization. Without a pre-oxidation process, the residual iron concentration varied from 12.42 to 13.95 mg/L, which decreased to values 0.02 to 0.08 mg/L when a pre-oxidation process was considered. As for arsenic, residual iron concentrations were also lower in the permeate generated by UFr membranes, differing significantly from the others generated in the UFs and UFp ($p<0.05$).

The primary mechanism associated with the removal of iron and arsenic was discussed in Chapter 2 (Section 1.7.1). Briefly, the circumstances favored the formation of insoluble complexes of iron and arsenic that could have co-precipitated. In this case, steric hindrance and size exclusion of these species, which have a size (up to 0.2 µm [46,56,57]) greater than the pores of the membrane, favors their removal. It should also be noted that the recycled membranes probably had pores smaller than

those conventionally observed for commercial UF membranes, which would contribute to the difference observed in terms of residual concentration.

Without a pre-oxidation, the UFr, UFs, and UFp were unable to attain the threshold values for manganese, with no significant difference between these systems. Residual manganese concentration ranged from 1.10 – 1.40 mg/L in experiments without pre-oxidation, regardless of the filtration system (UFr, UFs, and UFp) used and initial turbidity (100 – 1000 NTU). On the other hand, after pre-oxidation, the average manganese concentration in the UFs, UFp, and UFr (Figure 20c) permeate did not exceed the limit imposed by the World Health Organization (0.1 mg/L), with a few exceptions between the replicates of the experiments with UFs and UFp. Manganese complexes, when formed (MnO_2, Mn_2O_3, and Mn_3O_4, size: < 4.53 Å [106]), are often smaller than the pores of commercial UF membranes [31]. In that case, the effectiveness of UFr membranes becomes even more evident after a comparison between the residual concentration values for manganese (Figure 20c), achieving the lowest values among the three systems. Finally, the capacity of the UFr, UFs, and UFp to reject arsenic, iron, and manganese seems to be indifferent to the medium turbidity, with no significant differences being observed between the conditions of 100, 300, and 1000 NTU.

Figure 20. Residual concentration of arsenic, iron, and manganese in the permeate generated by UFs, UFp, and UFr, at different initial turbidities with feed spiked with 0.2 mg/L As, 25 mg/L Fe, 1.5 mg/L Mn (n=3). Letters in parentheses (a-l) show significantly different values within a specific physical-chemical parameter

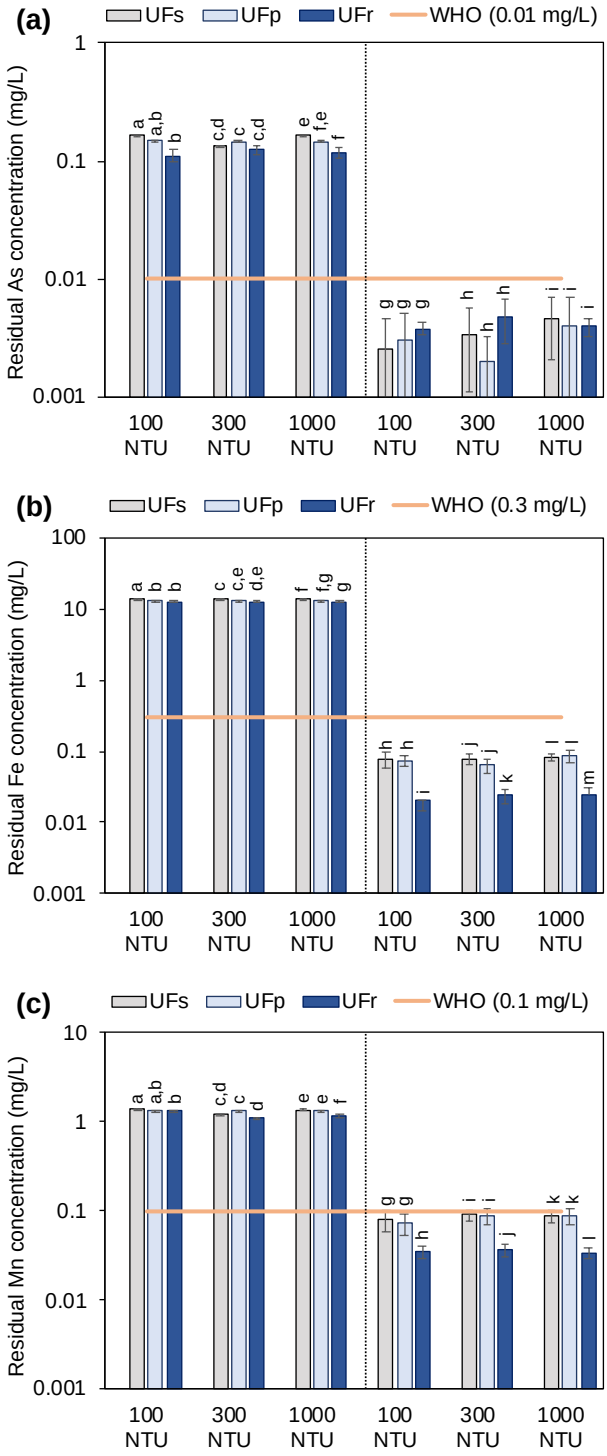

The results for turbidity and colour removal were summarized in Figure 21. There was no significant difference ($p > 0.173$) for turbidity or colour when the permeate with and without a pre-oxidation were compared, nor when different initial turbidity (100 – 1000 NTU) were compared for the same UF process (UFs, UFp, and UFr). The median

values for residual turbidity and colour complied with the threshold recommended by the World Health Organization for drinking water (turbidity: 1.0 NTU; colour: 15 uH [107]), which highlights the robustness of these processes for color and turbidity removal. Still, high initial turbidities combined with the occurrence of suspended matter can interfere in other operational variables, for example of permeate flux and fouling.

Figure 21. Residual (a) turbidity and (b) colour for the UFs, UFp and UFr permeate.

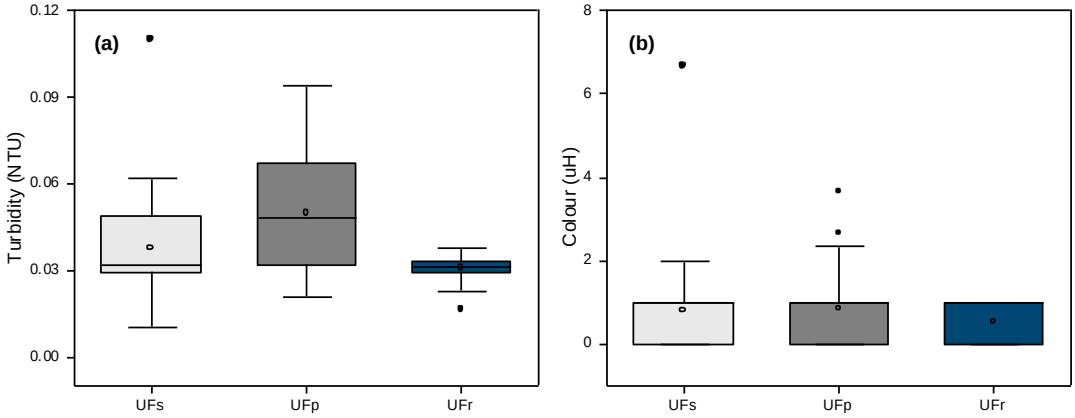

The permeate flux had no statistical difference with and without a pre-oxidation process. For that reason, the results related to the permeate flux, its decay (J/J_0), and permeate conductivity for the UFs, UFp, and UFr were summarized in Figure 22 for the experiments after pre-oxidation only.

The average permeate flux for UFs decreased from 106.0 ± 8.8 to 101.8 ± 12.1 L/m²h when the turbidity increased from 100 to 1000 NTU. The flux decay for these experiments differed significantly from each other ($H = 30.812$, $p<0.001$), noticing the lowest median of J/J_0 (0.69) for the experiment conducted at 1000 NTU. Similarly, the flux decay was also higher at 1000 NTU for UFp ($J/J_0 = 0.59$) and UFr ($J/J_0 = 0.66$), and differed significantly when compared to the J/J_0 obtained for 300 and 100 NTU. The average permeate flux for UFp corresponded to 185.2 ± 13.5 – 102.8 ± 28.8 L/m²h when the turbidity increased from 100 to 1000 NTU, whereas the values for UFr varied from 71.8 ± 5.2 – 65.2 ± 8.7 L/m²h for the same turbidity condition.

Despite the highest permeate flux, the J/J_0 value for UFp suggested that this configuration had also a higher propensity to fouling compared to UFs, also noticed by the higher fouling resistance reported in Table 11. UFp seems to be subjected to a more severe membrane fouling, especially under higher turbidity conditions, as

reported in previous studies [59,60]. For UFp, the compressibility and thickness of the cake layer formed tend to become more compact due to the external pressure applied, in most cases resulting in irreversible fouling after long-term operations.

Table 11. Membrane (*Rm*, 1/m), fouling (*Rf*, 1/m), and total (*Rt*, 1/m) resistances for UFs, UFp, and UFr filtration experiments.

	UFs			UFp			UFr		
	Rm	***Rf***	***Rt***	***Rm***	***Rf***	***Rt***	***Rm***	***Rf***	***Rt***
100 NTU		$7.27 \cdot 10^{11}$	$1.45 \cdot 10^{12}$		$7.50 \cdot 10^{11}$	$1.50 \cdot 10^{12}$		$6.13 \cdot 10^{12}$	$1.23 \cdot 10^{13}$
300 NTU	$7.27 \cdot 10^{11}$	$7.27 \cdot 10^{11}$	$1.45 \cdot 10^{12}$	$7.50 \cdot 10^{11}$	$7.50 \cdot 10^{11}$	$1.50 \cdot 10^{12}$	$6.13 \cdot 10^{12}$	$6.13 \cdot 10^{12}$	$1.23 \cdot 10^{13}$
1000 NTU		$7.27 \cdot 10^{11}$	$1.45 \cdot 10^{12}$		$7.50 \cdot 10^{11}$	$1.50 \cdot 10^{12}$		$6.13 \cdot 10^{12}$	$1.23 \cdot 10^{13}$

Compared to the UFp and UFs, UFr had the highest membrane and fouling resistance. The membrane itself has an average pore size and roughness, parameters inversely proportional to the membrane resistance, smaller if compared to the commercial UF membranes (section 3.2.4). That explains the results presented in Table 11 and the smaller permeate flux reported for UFr. In contrast, these are characteristics that favored the higher rejection rate for UFr previously mentioned, as well as the lower conductivity for the permeate as presented in Figure 22c. Moreover, a higher propensity for fouling not necessarily compromises the ion rejection capacity of UF-like membranes [108]. In some cases, it could even increase their efficiency to reject ions [109], mainly due to the formation of a gel-like layer on the membrane surface that can act as a dynamic barrier.

Figure 22. Permeate flux and conductivity for (a) UFs (0.2 bar), (b) UFp (0.4 bar) and (c) UFr (1 bar, 3.2 L/min) at different initial turbidities spiked with 0.2 mg/L As, 25 mg/L Fe, 1.5 mg/L Mn.

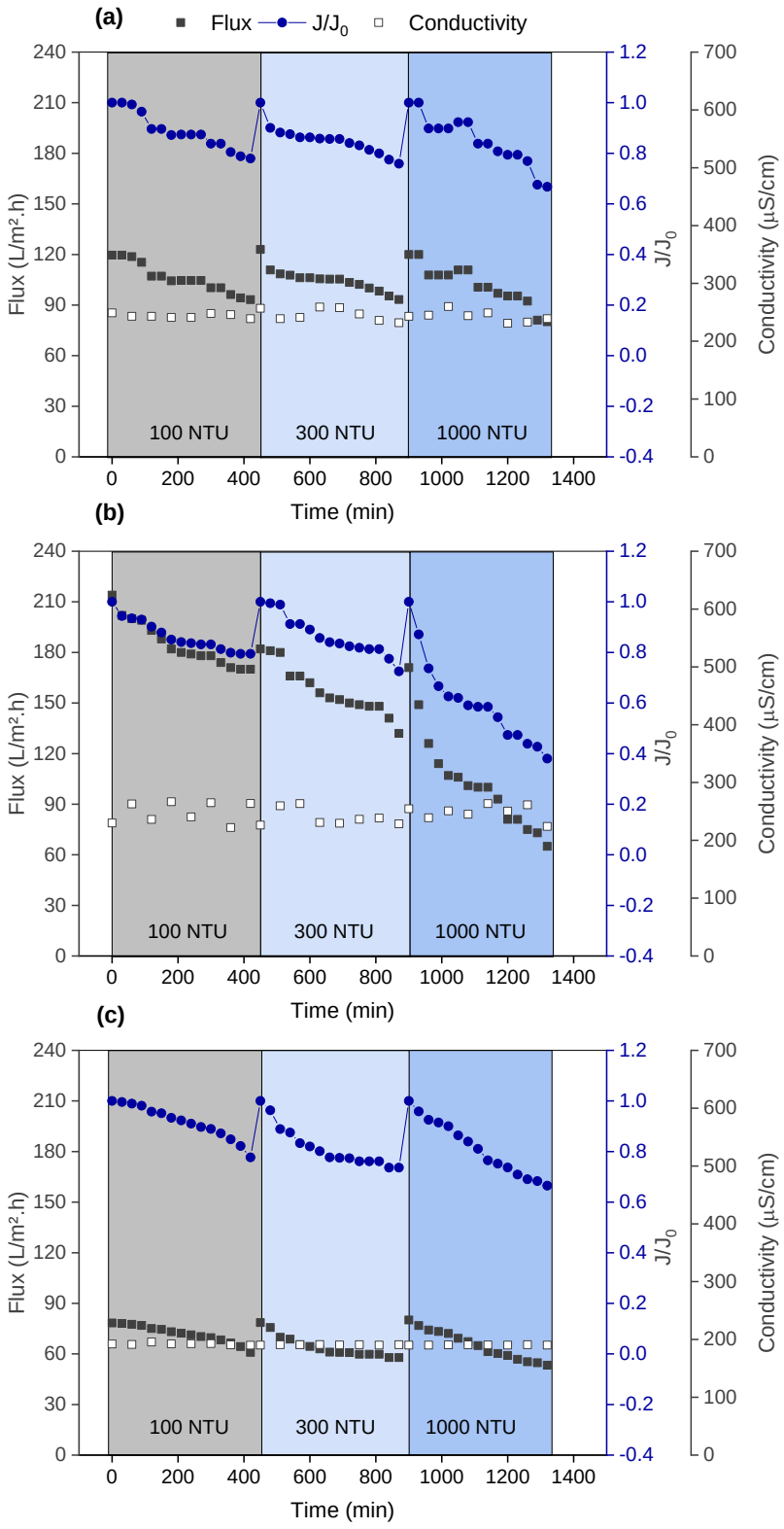

The results for the Hermia model fit are shown in Table 12, which allows for a better comprehension of the turbidity influence on the fouling mechanism. Although one fouling mechanism is generally associated with each case, other phenomena could

concomitantly occur. For a better interpretation of the results, the mechanisms described by Hermia were represented in Figure 23.

With an increase in turbidity, as in the case of UFs and UFr without pre-oxidation, it is noticeable that the predominant fouling mechanism goes from standard blockage (Figure 23c) to cake layer formation (Figure 23d). This change may be closely associated with an increase in the particle's concentration present in the medium that is likely to accumulate over the membrane surface causing the formation of a gel layer, which was previously unfavorable due to their lower concentration. For UFp, as this is an intrinsically more restricted module, it has, even at low levels of turbidity, the gel layer formation mechanism as the most prevalent fouling.

The pre-oxidation also influenced the predominant fouling phenomenon. The formation of insoluble compounds during the pre-oxidation can increase the solids content in the feed, which the propensity to the formation of a gel layer to be the predominant mechanism, this case can be observed for UFs 100 NTU. Another way of changing the mechanism may be the formation of larger precipitates, which would cause the change of the fouling mechanism for complete pore blocking, as in the case of UFp 300 NTU, for example.

Given the different types of membranes and modules, it can be seen that UFs and UFr have similar mechanisms of fouling when there is no pre-oxidation. Furthermore, in general, the "k" values from Hermia's model (which are higher when membrane fouling is more severe) for UFp are higher than UFr and UFs, in this order. This for systems without pre-oxidation, since the introduction of an oxidizing agent, alters the fouling mechanisms, changing the complexity of the medium and the physical and chemical phenomena that occur in the process.

Table 12. Permeation mass transfer coefficient correlated to k_s: standard blocking, k_i: intermediate blocking, k_{cl}: cake layer formation, and k_c: complete blocking, obtained from Hermia's model.

Water turbidity	Without pre-oxidation								Pre-oxidation							
	k_s ($1/m^{0.5}s^{0.5}$)	R^2	k_i (1/m)	R^2	k_{cl} (s/m^2)	R^2	k_c (1/s)	R^2	k_s ($1/m^{0.5}s^{0.5}$)	R^2	k_i (1/m)	R^2	k_{cl} (s/m^2)	R^2	k_c (1/s)	R^2
UFs																
100 NTU	$1.51\cdot10^{-3}$	**0.861**	$3.17\cdot10^{-6}$	0.860	$6.57\cdot10^{-8}$	0.859	$3.07\cdot10^{-4}$	0.842	$3.09\cdot10^{-3}$	0.940	$5.66\cdot10^{-6}$	0.938	$1.07\cdot10^{-7}$	**0.949**	$5.99\cdot10^{-4}$	0.930
300 NTU	$5.82\cdot10^{-3}$	0.929	$1.14\cdot10^{-5}$	0.941	$2.28\cdot10^{-7}$	**0.945**	$1.16\cdot10^{-3}$	0.934	$2.31\cdot10^{-3}$	0.838	$4.30\cdot10^{-6}$	0.862	$8.22\cdot10^{-8}$	**0.871**	$4.51\cdot10^{-4}$	0.847
1000 NTU	$7.66\cdot10^{-3}$	0.867	$2.33\cdot10^{-5}$	0.945	$4.91\cdot10^{-7}$	**0.970**	$2.27\cdot10^{-3}$	0.898	$2.10\cdot10^{-2}$	0.894	$8.67\cdot10^{-6}$	0.865	$1.78\cdot10^{-7}$	0.836	$8.55\cdot10^{-4}$	**0.914**
UFp																
100 NTU	$3.69\cdot10^{-3}$	0.877	$2.81\cdot10^{-6}$	0.895	$2.96\cdot10^{-8}$	**0.905**	$5.34\cdot10^{-4}$	0.884	$3.53\cdot10^{-3}$	0.930	$2.76\cdot10^{-6}$	0.948	$2.96\cdot10^{-8}$	**0.958**	$5.16\cdot10^{-4}$	0.936
300 NTU	$4.08\cdot10^{-3}$	0.925	$3.95\cdot10^{-6}$	0.935	$4.89\cdot10^{-8}$	**0.941**	$6.40\cdot10^{-4}$	0.929	$4.26\cdot10^{-3}$	0.937	$4.30\cdot10^{-6}$	0.939	$5.50\cdot10^{-8}$	0.932	$6.77\cdot10^{-4}$	**0.946**
1000 NTU	$1.02\cdot10^{-2}$	0.886	$1.82\cdot10^{-5}$	0.915	$3.52\cdot10^{-7}$	0.944	$1.94\cdot10^{-3}$	**0.947**	$9.76\cdot10^{-3}$	0.914	$1.92\cdot10^{-5}$	0.928	$4.05\cdot10^{-7}$	0.926	$1.92\cdot10^{-3}$	**0.960**
UFr																
100 NTU	$2.28\cdot10^{-3}$	**0.938**	$7.46\cdot10^{-6}$	0.910	$2.08\cdot10^{-7}$	0.888	$5.38\cdot10^{-4}$	0.930	$2.26\cdot10^{-3}$	**0.950**	$7.65\cdot10^{-6}$	0.923	$2.18\cdot10^{-7}$	0.902	$5.39\cdot10^{-4}$	0.942
300 NTU	$2.66\cdot10^{-3}$	0.854	$9.66\cdot10^{-5}$	**0.909**	$2.90\cdot10^{-7}$	0.889	$6.47\cdot10^{-4}$	0.866	$2.66\cdot10^{-3}$	0.852	$9.97\cdot10^{-6}$	0.888	$3.05\cdot10^{-7}$	**0.909**	$6.55\cdot10^{-4}$	0.864
1000 NTU	$4.05\cdot10^{-3}$	0.983	$1.51\cdot10^{-5}$	0.985	$4.98\cdot10^{-7}$	**0.987**	$9.94\cdot10^{-4}$	0.986	$4.00\cdot10^{-3}$	0.990	$1.54\cdot10^{-5}$	0.991	$4.81\cdot10^{-7}$	0.986	$9.93\cdot10^{-4}$	**0.992**

Figure 23. Representation of the different fouling mechanisms considered by Hermia's models. (a) complete blocking, (b) intermediate blocking, (c) standard blocking, and (d) cake layer formation.

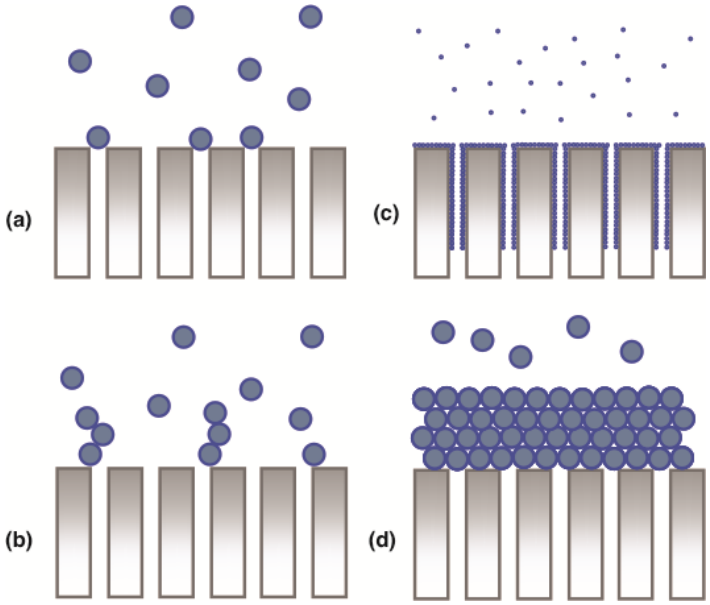

1.10.3 Comparison between conventional and UF treatment processes

A comparison between the conventional treatment with UF processes evidenced significant differences in terms of residual concentrations of arsenic, iron, and manganese ($p < 0.042$) (Figure 24). The instability of conventional processes is also noticed by the greatest data variability for the conventional treatment process. After sand filtration, only the residual concentration of iron was within the recommended for drinking water (0.3 mg/L). In terms of arsenic, 43% of the samples violated the recommended values for drinking water (0.01 mg/L), whereas all samples showed concentrations higher than that recommended for manganese (>0.1 mg/L). UF processes, on its turn, had median residual concentrations within the recommended values for all metal ions and metalloid.

On the other hand, removal of turbidity and color (Figure 25) does not appear to be a limitation of conventional treatment processes since they were within their threshold values. Even so, the values obtained for these two parameters (turbidity and colour) were higher than those observed for UF processes, which reinforces their ability to guarantee a safe drinking water supply.

Figure 24. Comparison between conventional treatment (CT), UFs, UFp, and UFr, for the residual concentration of arsenic, iron, and manganese. Feed at 100-1000 NTU spiked with 0.2 mg/L As, 25 mg/L Fe, 1.5 mg/L Mn.

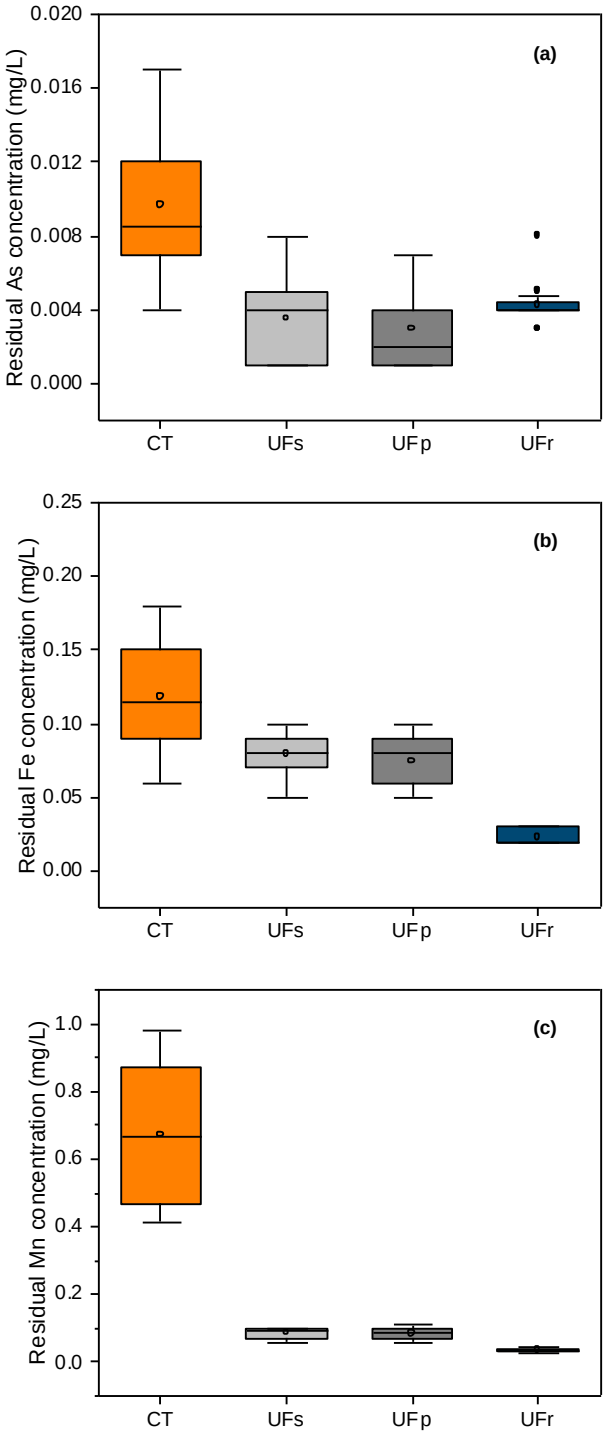

Figure 25. Comparison between conventional treatment (CT), UFs, UFp, and UFr, for the residual values of turbidity and colour. Feed at 100-1000 NTU spiked with 0.2 mg/L As, 25 mg/L Fe, 1.5 mg/L Mn.

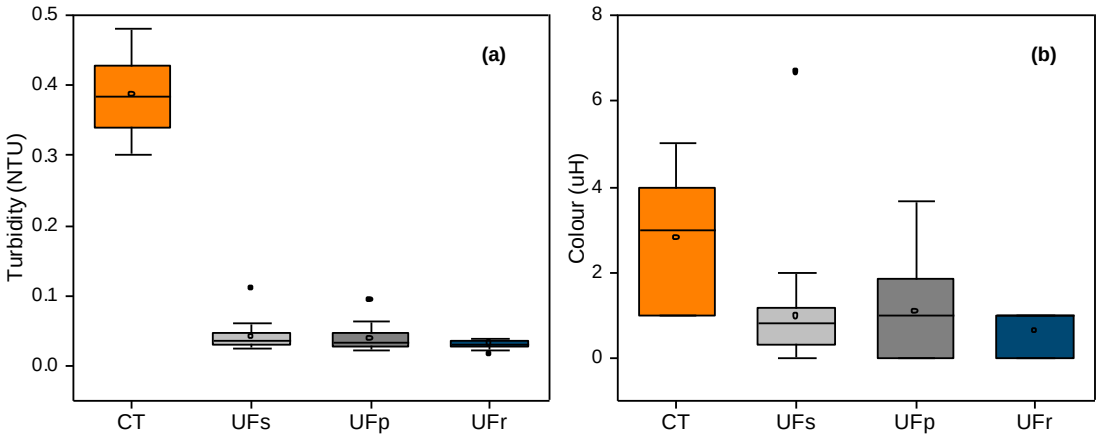

Another important aspect, besides the process efficiency, is the waste generation in each process. In the conventional water treatment, a considerable amount of sludge is generated in addition to the large volume of water that is used for the backwashing of sand filters. It is estimated that a typical drinking water treatment plant generates about 100,000 tons of sludge yearly [110]. In UF processes, although there is a production of a concentrate stream, the volume of waste generated is lower since it is common to operate UF systems with recovery rates up to 95%. Nevertheless, not only do these aspects make UF systems advantageous, but also their operational simplicity, modularity, operational predictability (since they are physical separation processes), and also the opportunity for their implementation and use in decentralized systems with the eventual coupling with renewable energy.

1.11 Economic analysis

The main economic components related to UFr, UFs, and UFp are shown in **Erro! Fonte de referência não encontrada.**, and their full description in Table 13.

Figure 26. (a) Economic analysis comparison for UFs, UFp, and UFr, for a feed flow rate of 10.8 m^3/h and (b) costs breakdown for UFr at different treatment capacities.

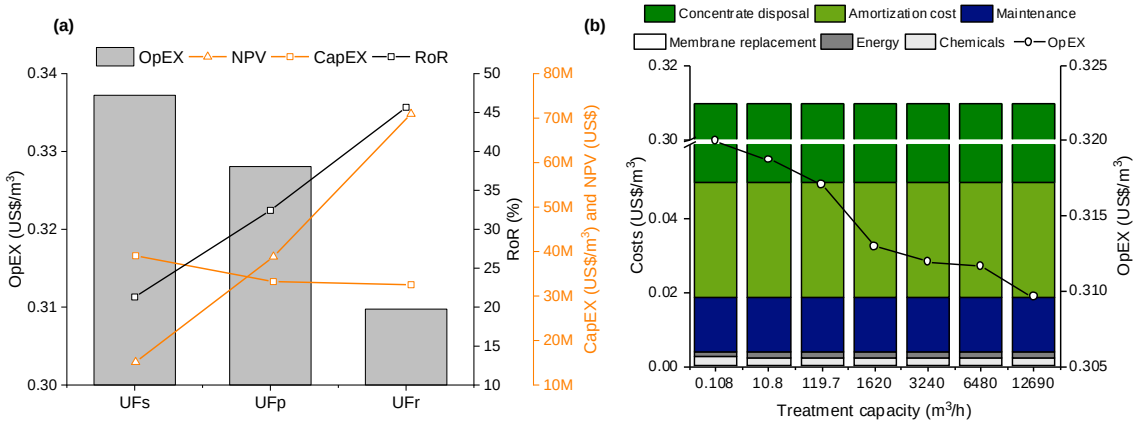

Table 13. Operating expenditures (per year) breakdown for all the UF systems.

	0.108 m³/h	10.8 m³/h	119.7 m³/h	1,620 m³/h	3,240 m³/h	6,480 m³/h	12,690 m³/h
				UFs			
Membrane replacement (US$/y)	25.46	2,200.62	23,810.66	302,812.24	572,888.02	1,069,390.96	2,072,854.34
Chemicals (US$/y)	2.03	202.85	2,248.22	30,426.97	60,853.95	121,707.89	238,344.63
Energy (US$/y)	1.42	141.91	1,572.86	21,286.80	42,573.60	85,147.20	166,746.60
Maintenance (US$/y)	16.62	1,661.54	18,415.38	249,230.77	498,461.54	996,923.08	1,952,307.69
Amortization cost (US$/y)	35.34	3,534.18	39,170.55	530,127.72	1,060,255.44	2,120,510.87	4,152,667.13
Concentrate disposal (US$/y)	245.98	24,598.08	272,628.72	3,689,712.00	7,379,424.00	14,758,848.00	28,902,744.00
Annual expenditures (US$/y)	326.85	32,339.18	357,846.38	4,823,596.50	9,614,456.54	19,152,528.01	37,485,664.38
OpEX (US$/m³)	0.345	0.342	0.341	0.34	0.339	0.337	0.337
CapEX (US$)	332.31	33,230.77	368,307.69	4,984,615.38	9,969,230.77	19,938,461.54	39,046,153.85
Payback (y)	2	2	2	2	2	2	2
NPV (US$)	1,259.07	96,450.32	816,766.37	3,145,344.83	4,305,399.71	8,926,540.28	15,141,649.97
RoR (%)	65.94	54.82	46.14	24.92	21.97	22.21	21.3
				UFp			
Membrane replacement (US$/y)	25.46	2,200.62	23,810.66	302,812.24	572,888.02	1,069,390.96	2,116,957.62
Chemicals (US$/y)	2.03	202.85	2,248.22	30,426.97	60,853.95	121,707.89	243,415.79
Energy (US$/y)	1.42	141.91	1,572.86	21,286.80	42,573.60	85,147.20	170,294.40
Maintenance (US$/y)	13.85	1,384.62	15,346.15	207,692.31	415,384.62	830,769.23	1,661,538.46
Amortization cost (US$/y)	29.45	2,945.15	32,642.12	441,773.10	883,546.20	1,767,092.39	3,534,184.79
Concentrate disposal (US$/y)	245.98	24,598.08	272,628.72	3,689,712.00	7,379,424.00	14,758,848.00	29,517,696.00
Annual expenditures (US$/y)	318.19	31,473.23	348,248.73	4,693,703.42	9,354,670.38	18,632,955.68	37,244,087.06
OpEX (US$/m³)	0.336	0.333	0.332	0.331	0.330	0.328	0.328
CapEX (US$)	276.92	27,692.31	885,780.00	4,153,846.15	8,307,692.31	16,615,384.62	33,230,769.23

	0.108 m³/h	**10.8 m³/h**	**119.7 m³/h**	**1,620 m³/h**	**3,240 m³/h**	**6,480 m³/h**	**12,690 m³/h**
Payback (y)	2	2	2	2	2	2	2
NPV (US$)	1,453.81	115,924.22	1,032,602.08	6,066,429.70	10,147,569.44	20,610,879.75	38,832,491.67
RoR (%)	84.15	70.90	60.63	36.33	33.14	33.39	32.42
				UFr			
Membrane replacement (US$/y)	0.38	32.01	314.45	3,737.41	7,092.90	13,967.56	27,139.43
Chemicals (US$/y)	2.03	202.85	2,248.22	30,426.97	60,853.95	121,707.89	238,344.63
Energy (US$/y)	1.42	141.91	1,572.86	21,286.80	42,573.60	85,147.20	166,746.60
Maintenance (US$/y)	13.85	1,384.62	15,346.15	207,692.31	415,384.62	830,769.23	1,626,923.08
Amortization cost (US$/y)	29.45	2,945.15	32,642.12	441,773.10	883,546.20	1,767,092.39	3,460,555.94
Concentrate disposal (US$/y)	245.98	24,598.08	272,628.72	3,689,712.00	7,379,424.00	14,758,848.00	28,902,744.00
Annual expenditures (US$/y)	293.10	29,304.62	324,752.52	4,394,628.59	8,788,875.26	17,577,532.27	34,422,453.68
OpEX (US$/m³)	0.320	0.319	0.317	0.313	0.312	0.312	0.310
CapEX (US$)	276.92	27,692.31	306,923.08	4,153,846.15	8,307,692.31	16,615,384.62	32,538,461.54
Payback (y)	2	2	2	2	2	2	2
NPV (US$)	1,857.46	150,822.74	1,410,716.81	10,879,317.16	19,252,676.26	37,595,372.16	70,944,325.33
RoR (%)	102.28	86.60	76.01	51.25	47.42	46.72	45.66

Compared with UFs, UFp had a lower CapEX and OpEX. Despite the advantages of higher permeate flux, and therefore lower membrane area requirements, UFp has generally a shorter lifespan (due to the increased fouling propensity and thus, higher cleaning frequency [60]) which represents a higher cost for membrane replacement. Still, the longer lifespan of UFs and higher permeate flux for UFp, both compared to UFr, did not compensated the lower membrane costs related to UFr. Due to that fact, UFr had the lower OpEX among all three systems assessed, whereas UFs had the highest OpEX among them. Treatment costs were still lower than those presented for the conventional treatment route. From previous studies, the cost associated with the conventional water treatment ranges from 0.2 US$/$m^3$ to 0.9 US$/$m^3$ varying accordingly with the treatment capacity [77].

Comparing UFs to UFr, it can be seen that UFr has a lower CapEX and OpEX. The lower membrane costs for UFr offset the higher energy requirements and lower permeate flux that this system presents. This system accounted with recycled membranes also showed a higher value for UFr compared to the others, which reaffirms its long-term economic viability. This result is in line with the technical feasibility of this system, since, among those evaluated, UFr was the one that showed the highest removal efficiencies for arsenic, iron, and manganese. Notwithstanding, the payback period for this system is calculated to be 2 years.

Considering that the UFr system is better in technical and economic aspects, a sensitive analysis considering different feed flow rates was performed (Figure 26b), it can be noticed that the OpEX decreases with an increase in the treatment capacity of the drinking water facility. Among these components, the cost associated with membrane replacement is currently one of the most expensive components when it comes to treatment processes using membranes, somewhat aggravated due to the reduced lifespan of these UFr membranes (2 years) compared to commercially available UF membranes (5 – 7 years).

The advantages of a recycled membrane system also extend to environmental aspects. De Paula & Amaral [61] indicated that a chemical conversion of a RO membrane could result in 2,609.81 kg of materials not being simply disposed of in landfills or withdrawn from the environment. The authors still demonstrated that the recycling of 9000 annual elements could represent monetary savings up to US$

10,469,070 and a total saved material of 84,150 kg/year. The results presented by De Paula & Amaral [61] and those reported in the current study reinforces the idea that an UFr system allows for economic gains, which can be associated with environmental benefits.

CHAPTER 4

FINAL CONSIDERATIONS

Drinking water treatment plants based on conventional treatment processes were not designed for arsenic removal. Although adverse conditions of colour and turbidity in raw surface water were not a problem, the increased concentration of arsenic and manganese represents a major concern, an issue possible to overcome after the implementation of a pre-oxidation process and the membrane systems, which allowed for higher robustness and compliance with legislation limits. The contribution of the pre-oxidation was highlighted, which corroborated the formation of insoluble complexes with a diameter higher than these membranes' pore size. Different UF membranes were also integrated to pre-oxidation in an alternative treatment process. Among them, UFr has a lower flux and higher flux decay than the other systems, the cost associated with the membrane acquisition contributed to the lowest OpEX (0.310 US$/m^3) among all systems (OpEX 0.337 and 0.328 US$/m^3 for UFs and UFp respectively), in addition to a higher RoR (45.66%). Besides the UF processes efficiency, a considerable amount of waste generation derived from conventional coagulation-flocculation would be avoided compared to conventional water treatment processes. Complementarily, for being an affordable technology, the use of UFr membranes would meet a first pre-requisite for novel technologies being sought for a safe drinking water supply. The outcome could be a reliable water service in terms of quantity and/or quality and an alternative to the improvement of existing centralized drinking water facilities, often prohibitively costly and time-consuming. Extending the use of UFr, therefore, could reduce the gap between the water demand and its supply observed over the past decades, as a decentralized drinking water technology.

CHAPTER 5

REFERENCES

[1] V.R. Moreira, Y.A.R. Lebron, L.V.S. Santos, E. Coutinho de Paula, M.C.S. Amaral, Arsenic contamination, effects and remediation techniques: A special look onto membrane separation processes, Process Saf. Environ. Prot. 148 (2021) 604–623. https://doi.org/10.1016/j.psep.2020.11.033.

[2] J. Podgorski, M. Berg, Global threat of arsenic in groundwater, Science (80-.). 368 (2020) 845–850. https://doi.org/10.1126/science.aba1510.

[3] M.S. Sankar, M.A. Vega, P.P. Defoe, M.G. Kibria, S. Ford, K. Telfeyan, A. Neal, T.J. Mohajerin, G.M. Hettiarachchi, S. Barua, C. Hobson, K. Johannesson, S. Datta, Elevated arsenic and manganese in groundwaters of Murshidabad, West Bengal, India, Sci. Total Environ. 488–489 (2014) 570–579. https://doi.org/10.1016/j.scitotenv.2014.02.077.

[4] Z. Zhang, C. Xiao, O. Adeyeye, W. Yang, X. Liang, Source and Mobilization Mechanism of Iron, Manganese and Arsenic in Groundwater of Shuangliao City, Northeast China, Water. 12 (2020) 534. https://doi.org/10.3390/w12020534.

[5] C. Hopenhayn-Rich, M. Lou Biggs, A.H. Smith, Lung and kidney cancer mortality associated with arsenic in drinking water in Cordoba, Argentina, Int. J. Epidemiol. 27 (1998) 561–569. https://doi.org/10.1093/ije/27.4.561.

[6] D.N.G. Mazumder, J. Das Gupta, A. Santra, A. Pal, A. Ghose, S. Sarkar, N. Chattopadhaya, D. Chakraborti, Non-cancer effects of chronic arsenicosis with special reference to liver damage, in: Arsenic, Springer Netherlands, Dordrecht, 1997: pp. 112–123. https://doi.org/10.1007/978-94-011-5864-0_10.

[7] A.H. Milton, Z. Hasan, A. Rahman, M. Rahman, Chronic arsenic poisoning and respiratory effects in Bangladesh, J. Occup. Health. 43 (2001) 136–140. https://doi.org/10.1539/joh.43.136.

[8] L. Gerhardsson, E. Dahlgren, A. Eriksson, B.E.A. Lagerkvist, J. Lundstrom, G.F. Nordberg, Fatal arsenic poisoning - A case report, Scand. J. Work. Environ. Heal. 14 (1988) 130–133. https://doi.org/10.5271/sjweh.1944.

[9] S.M.Z. Naqvi, C. Vaishnavi, H. Singh, Toxicity and Metabolism of Arsenic in

Vertebrates, Arsen. Environ. Part II Hum. Heal. Ecosyst. Eff. (1994) 55–90.

[10] D.N. Guha Mazumder, Arsenic and liver disease., J. Indian Med. Assoc. 99 (2001) 311, 314–5, 318–20.

[11] A. Santra, A. Maiti, S. Das, S. Lahiri, S.K. Charkaborty, D.N. Guha Mazumder, Hepatic damage caused by chronic arsenic toxicity in experimental animals, J. Toxicol. - Clin. Toxicol. 38 (2000) 395–405. https://doi.org/10.1081/CLT-100100949.

[12] A. Santra, J. Das Gupta, B.K. De, B. Roy, D.N. Guha Mazumder, Hepatic manifestations in chronic arsenic toxicity, Indian J. Gastroenterol. 18 (1999) 152–155.

[13] S.K. Bansal, N. Haldar, U.K. Dhand, J.S. Chopra, Phrenic neuropathy in arsenic poisoning, Chest. 100 (1991) 878–880. https://doi.org/10.1378/chest.100.3.878.

[14] P.N. Chhuttani, L.S. Chawla, T.D. Sharma, Arsenical neuropathy, Neurology. 17 (1967) 269–274. https://doi.org/10.1212/wnl.17.3.269.

[15] S.L. Wagner, J.S. Maliner, W.E. Morton, R.S. Braman, Skin Cancer and Arsenical Intoxication From Well Water, Arch. Dermatol. 115 (1979) 1205–1207. https://doi.org/10.1001/archderm.1979.04010100025010.

[16] D.A. Grantham, J.F. Jones, Arsenic contamination of water wells in Nova Scotia, J. / Am. Water Work. Assoc. 69 (1977) 653–657. https://doi.org/10.1002/j.1551-8833.1977.tb06844.x.

[17] R.E. Gerhardt, J.B. Hudson, R.N. Rao, R.E. Sobel, Chronic Renal Insufficiency From Cortical Necrosis Induced by Arsenic Poisoning, Arch. Intern. Med. 138 (1978) 1267–1269. https://doi.org/10.1001/archinte.1978.03630330067019.

[18] Y. Shiobara, Y. Ogra, K.T. Suzuki, Animal species difference in the uptake of dimethylarsinous acid (DMAIII) by red blood cells, Chem. Res. Toxicol. 14 (2001) 1446–1452. https://doi.org/10.1021/tx015537k.

[19] K.S. Squibb, B.A. Fowler, The toxicity of arsenic and its compounds, in: Biol.

Environ. Eff. Arsen., Elsevier, 1983: pp. 233–269. https://doi.org/10.1016/b978-0-444-80513-3.50011-6.

[20] A. Léonard, R.R. Lauwerys, Carcinogenicity, teratogenicity and mutagenicity of arsenic, Mutat. Res. Genet. Toxicol. 75 (1980) 49–62. https://doi.org/10.1016/0165-1110(80)90027-5.

[21] V. Bencko, V. Wagner, M. Wagnerová, J. Bátora, Immunological profiles in workers of a power plant burning coal rich in arsenic content., J. Hyg. Epidemiol. Microbiol. Immunol. 32 (1988) 137–146. http://www.ncbi.nlm.nih.gov/pubmed/2457611.

[22] E. Astolfi, A. Maccagno, J.C. García Fernández, R. Vaccaro, R. Stímola, Relation between arsenic in drinking water and skin cancer, Biol. Trace Elem. Res. 3 (1981) 133–143. https://doi.org/10.1007/BF02990453.

[23] S.L. O'Neal, W. Zheng, Manganese Toxicity Upon Overexposure: a Decade in Review, Curr. Environ. Heal. Reports. 2 (2015) 315–328. https://doi.org/10.1007/s40572-015-0056-x.

[24] J. Crossgrove, W. Zheng, Manganese toxicity upon overexposure, NMR Biomed. 17 (2004) 544–553. https://doi.org/10.1002/nbm.931.

[25] J.P. Vareda, A.J.M. Valente, L. Durães, Assessment of heavy metal pollution from anthropogenic activities and remediation strategies: A review, J. Environ. Manage. 246 (2019) 101–118. https://doi.org/10.1016/j.jenvman.2019.05.126.

[26] D.T. Moussa, M.H. El-Naas, M. Nasser, M.J. Al-Marri, A comprehensive review of electrocoagulation for water treatment: Potentials and challenges, J. Environ. Manage. 186 (2017) 24–41. https://doi.org/10.1016/j.jenvman.2016.10.032.

[27] C. Zhao, J. Zhou, Y. Yan, L. Yang, G. Xing, H. Li, P. Wu, M. Wang, H. Zheng, Application of coagulation/flocculation in oily wastewater treatment: A review, Sci. Total Environ. 765 (2021) 142795. https://doi.org/10.1016/j.scitotenv.2020.142795.

[28] G. Pavanelli, Eficiência de diferentes tipos de coagulantes na coagulação,

floculação e sedimentação de água com cor ou turbidez elevada, Universidade Federal de São Carlos, 2001.

[29] L. Di Bernardo, Â.D.B. Dantas, Métodos e técnicas de tratamento de água, Eng. Sanit. e Ambient. 11 (2006) 107–107. https://doi.org/10.1590/S1413-41522006000200001.

[30] L.C. Konradt-Moraes, Estudo dos processos de coagulação e floculação seguidos de filtração com membranas para a obtenção de água potável, Universidade Estadual de Maringá, 2004.

[31] M. Libânio, Fundamentos de Qualidade e Tratamento de Água, 4th ed., 2016.

[32] E.W. Steel, Abastecimento de Água - Sistema de Esgotos, Livro Técnico S. A., Rio de Janeiro, Brasil, 1966.

[33] I. Krupińska, Aluminium drinking water treatment residuals and their toxic impact on human health, Molecules. 25 (2020) 641. https://doi.org/10.3390/molecules25030641.

[34] J.K. Edzwald, Aluminum in Drinking Water: Occurrence, Effects, and Control, J. AWWA. 112 (2020) 34–41. https://doi.org/10.1002/awwa.1499.

[35] W.L. Ang, A.W. Mohammad, State of the art and sustainability of natural coagulants in water and wastewater treatment, J. Clean. Prod. 262 (2020) 121267. https://doi.org/10.1016/j.jclepro.2020.121267.

[36] M. Lv, Z. Zhang, J. Zeng, J. Liu, M. Sun, R.S. Yadav, Y. Feng, Roles of magnetic particles in magnetic seeding coagulation-flocculation process for surface water treatment, Sep. Purif. Technol. 212 (2019) 337–343. https://doi.org/10.1016/j.seppur.2018.11.011.

[37] K. Mandel, F. Hutter, C. Gellermann, G. Sextl, Reusable superparamagnetic nanocomposite particles for magnetic separation of iron hydroxide precipitates to remove and recover heavy metal ions from aqueous solutions, Sep. Purif. Technol. 109 (2013) 144–147. https://doi.org/10.1016/j.seppur.2013.03.002.

[38] A.B. Şengül, G. Ersan, N. Tüfekçi, Removal of intra- and extracellular microcystin by submerged ultrafiltration (UF) membrane combined with coagulation/flocculation and powdered activated carbon (PAC) adsorption, J. Hazard. Mater. 343 (2018) 29–35. https://doi.org/10.1016/j.jhazmat.2017.09.018.

[39] R. Bouchareb, K. Derbal, Y. Özay, Z. Bilici, N. Dizge, Combined natural/chemical coagulation and membrane filtration for wood processing wastewater treatment, J. Water Process Eng. 37 (2020) 101521. https://doi.org/10.1016/j.jwpe.2020.101521.

[40] J.C. Crittenden, R.R. Trussell, D.W. Hand, K.J. Howe, G. Tchobanoglous, Principles and Design, 3rd ed., John Wiley & Sons, 2012. http://doi.wiley.com/10.1002/9781118131473.

[41] D. Vries, C. Bertelkamp, F. Schoonenberg Kegel, B. Hofs, J. Dusseldorp, J.H. Bruins, W. de Vet, B. van den Akker, Iron and manganese removal: Recent advances in modelling treatment efficiency by rapid sand filtration, Water Res. 109 (2017) 35–45. https://doi.org/10.1016/j.watres.2016.11.032.

[42] H. Yang, Z. Yan, X. Du, L. Bai, H. Yu, A. Ding, G. Li, H. Liang, T.M. Aminabhavi, Removal of manganese from groundwater in the ripened sand filtration: Biological oxidation versus chemical auto-catalytic oxidation, Chem. Eng. J. 382 (2020) 123033. https://doi.org/10.1016/j.cej.2019.123033.

[43] Y. Guo, L. Bai, X. Tang, Q. Huang, B. Xie, T. Wang, J. Wang, G. Li, H. Liang, Coupling continuous sand filtration to ultrafiltration for drinking water treatment: Improved performance and membrane fouling control, J. Memb. Sci. 567 (2018) 18–27. https://doi.org/10.1016/j.memsci.2018.09.034.

[44] D. Xu, L. Bai, X. Tang, D. Niu, X. Luo, X. Zhu, G. Li, H. Liang, A comparison study of sand filtration and ultrafiltration in drinking water treatment: Removal of organic foulants and disinfection by-product formation, Sci. Total Environ. 691 (2019) 322–331. https://doi.org/10.1016/j.scitotenv.2019.07.071.

[45] S. Sorlini, F. Gialdini, M.C. Collivignarelli, Survey on full-scale drinking water

treatment plants for arsenic removal in Italy, Water Pract. Technol. 9 (2014) 42–51. https://doi.org/10.2166/wpt.2014.005.

[46] M. Bauer, C. Blodau, Arsenic distribution in the dissolved, colloidal and particulate size fraction of experimental solutions rich in dissolved organic matter and ferric iron, Geochim. Cosmochim. Acta. 73 (2009) 529–542. https://doi.org/10.1016/j.gca.2008.10.030.

[47] M. Bissen, F.H. Frimmel, Arsenic— a Review. Part II: Oxidation of Arsenic and its Removal in Water Treatment, Acta Hydrochim. Hydrobiol. 31 (2003) 97–107. https://doi.org/10.1002/aheh.200300485.

[48] S. Sorlini, F. Gialdini, Conventional oxidation treatments for the removal of arsenic with chlorine dioxide, hypochlorite, potassium permanganate and monochloramine, Water Res. 44 (2010) 5653–5659. https://doi.org/10.1016/j.watres.2010.06.032.

[49] L.H. Andrade, A.O. Aguiar, W.L. Pires, G.A. Miranda, M.C.S. Amaral, Integrated ultrafiltration-nanofiltration membrane processes applied to the treatment of gold mining effluent: Influence of feed pH and temperature, Sep. Sci. Technol. 52 (2017) 756–766. https://doi.org/10.1080/01496395.2016.1262419.

[50] M.C.S. Amaral, L.B. Grossi, R.L. Ramos, B.C. Ricci, L.H. Andrade, Integrated UF–NF–RO route for gold mining effluent treatment: From bench-scale to pilot-scale, Desalination. 440 (2018) 111–121. https://doi.org/10.1016/j.desal.2018.02.030.

[51] B.G. Reis, A.L.B. Araújo, M.C.S. Amaral, H.C. Ferraz, Comparison of Nanofiltration and Direct Contact Membrane Distillation as an alternative for gold mining effluent reclamation, Chem. Eng. Process. - Process Intensif. 133 (2018) 24–33. https://doi.org/10.1016/j.cep.2018.08.020.

[52] B. Teychene, G. Collet, H. Gallard, J.P. Croue, A comparative study of boron and arsenic (III) rejection from brackish water by reverse osmosis membranes, Desalination. 310 (2013) 109–114. https://doi.org/10.1016/j.desal.2012.05.034.

[53] A.F.S. Foureaux, Y.A.R. Lebron, V.R. Moreira, L.B. Grossi, L.V.S. Santos, M.C.S. Amaral, Technical and economic potential of high-temperature NF and DCMD for gold mining effluent reclamation, Chem. Eng. Res. Des. 162 (2020) 149–161. https://doi.org/10.1016/j.cherd.2020.08.003.

[54] A. Ahmad, S. Rutten, L. de Waal, P. Vollaard, C. van Genuchten, H. Bruning, E. Cornelissen, A. van der Wal, Mechanisms of arsenate removal and membrane fouling in ferric based coprecipitation–low pressure membrane filtration systems, Sep. Purif. Technol. 241 (2020) 116644. https://doi.org/10.1016/j.seppur.2020.116644.

[55] S. Fendorf, H.A. Michael, A. van Geen, Spatial and Temporal Variations of Groundwater Arsenic in South and Southeast Asia, Science (80-.). 328 (2010) 1123–1127. https://doi.org/10.1126/science.1172974.

[56] K. Ritter, R. Aiken, George, J.F. Ranville, M. Bauer, D.L. Macalady, Evidence for the Aquatic Binding of Arsenate by Natural Organic Matter−Suspended Fe(III), Environ. Sci. Technol. 40 (2006) 5380–5387. https://doi.org/10.1021/es0519334.

[57] C.J. Tadanier, M.E. Schreiber, J.W. Roller, Arsenic Mobilization through Microbially Mediated Deflocculation of Ferrihydrite, Environ. Sci. Technol. 39 (2005) 3061–3068. https://doi.org/10.1021/es048206d.

[58] E. Drioli, M. Nakagaki, eds., Membranes and Membrane Processes, Springer US, Boston, MA, 1986. https://doi.org/10.1007/978-1-4899-2019-5.

[59] Y.-J. Kim, J.-W. Jung, S. Lee, Comparison of fouling rates for pressurized and submerged ultrafiltration membranes, Desalin. Water Treat. 54 (2015) 3610–3615. https://doi.org/10.1080/19443994.2014.923208.

[60] S.-R. Chae, H. Yamamura, B. Choi, Y. Watanabe, Fouling characteristics of pressurized and submerged PVDF (polyvinylidene fluoride) microfiltration membranes in a pilot-scale drinking water treatment system under low and high turbidity conditions, Desalination. 244 (2009) 215–226. https://doi.org/10.1016/j.desal.2008.05.025.

[61] E. Coutinho de Paula, M.C. Santos Amaral, Environmental and economic evaluation of end-of-life reverse osmosis membranes recycling by means of chemical conversion, J. Clean. Prod. 194 (2018) 85–93. https://doi.org/10.1016/j.jclepro.2018.05.099.

[62] E. Coutinho de Paula, J.C.L. Gomes, M.C.S. Amaral, Recycling of end-of-life reverse osmosis membranes by oxidative treatment: a technical evaluation, Water Sci. Technol. 76 (2017) 605–622. https://doi.org/10.2166/wst.2017.238.

[63] J. Gregor, Arsenic removal during conventional aluminium-based drinking-water treatment, Water Res. 35 (2001) 1659–1664. https://doi.org/10.1016/S0043-1354(00)00424-3.

[64] W.H.O. WHO, Potable Reuse: Guidance for producing safe drinking-water, 2017.

[65] J.G. Hering, P.-Y. Chen, J.A. Wilkie, M. Elimelech, S. Liang, Arsenic removal by ferric chloride, J. Am. Water Works Assoc. 88 (1996) 155–167. https://doi.org/10.1002/j.1551-8833.1996.tb06541.x.

[66] L.B. Grossi, C.B. Alvim, C.M.S. Alvares, M.F. Martins, M.C.S. Amaral, Purifying surface water contaminated with industrial failure using direct contact membrane distillation, Sep. Purif. Technol. 233 (2020) 116052. https://doi.org/10.1016/j.seppur.2019.116052.

[67] C.F. Couto, A.V. Santos, M.C.S. Amaral, L.C. Lange, L.H. de Andrade, A.F.S. Foureaux, B.S. Fernandes, Assessing potential of nanofiltration, reverse osmosis and membrane distillation drinking water treatment for pharmaceutically active compounds (PhACs) removal, J. Water Process Eng. 33 (2020) 101029. https://doi.org/10.1016/j.jwpe.2019.101029.

[68] M. Pascual-Benito, P. Emiliano, R. Casas-Mangas, C. Dacal-Rodríguez, M. Gracenea, R. Araujo, F. Valero, C. García-Aljaro, F. Lucena, Assessment of dead-end ultrafiltration for the detection and quantification of microbial indicators and pathogens in the drinking water treatment processes, Int. J. Hyg. Environ. Health. 230 (2020) 113628. https://doi.org/10.1016/j.ijheh.2020.113628.

[69] W.H.O. WHO, Water Quality and Health - Review of Turbidity: Information for regulators and water suppliers, 2017.

[70] G.S. Bilotta, R.E. Brazier, Understanding the influence of suspended solids on water quality and aquatic biota, Water Res. 42 (2008) 2849–2861. https://doi.org/10.1016/j.watres.2008.03.018.

[71] M.C. Teixeira, A.C. Santos, C.S. Fernandes, J.C. Ng, Arsenic contamination assessment in Brazil – Past, present and future concerns: A historical and critical review, Sci. Total Environ. 730 (2020) 138217. https://doi.org/10.1016/j.scitotenv.2020.138217.

[72] G. Hu, H.R. Mian, R. Dyck, M. Mohseni, S. Jasim, K. Hewage, R. Sadiq, Drinking Water Treatments for Arsenic and Manganese Removal and Health Risk Assessment in White Rock, Canada, Expo. Heal. (2019). https://doi.org/10.1007/s12403-019-00338-4.

[73] APHA, Standard Methods for the Examination of Water and Wastewater (23th ed.), 2017.

[74] R.W. Fox, A.T. McDonald, Introduction to Fluid Mechanics, 8th ed., Wiley, 2011. https://doi.org/10.1080/03043799408928334.

[75] R. Turton, R.C. Bailie, Analysis, Synthesis, and Design of Chemical Processes, 4th ed., Prentice Hall, 2012.

[76] B.C. do B. BACEN, Taxa de juros nominal - Overnight / Selic, (2021). http://www.ipeadata.gov.br/exibeserie.aspx?serid=38402.

[77] M.R. Wiesner, J. Hackney, S. Sethi, J.G. Jacangelo, J.-M. Laîé, Cost estimates for membrane filtration and conventional treatment, J. Am. Water Works Assoc. 86 (1994) 33–41. https://doi.org/10.1002/j.1551-8833.1994.tb06284.x.

[78] CEMIG, Valores de tarigas e serviços, (2021). https://www.cemig.com.br/atendimento/valores-de-tarifas-e-servicos/.

[79] J. Li, S. Jiao, L. Zhong, J. Pan, Q. Ma, Optimizing coagulation and flocculation

process for kaolinite suspension with chitosan, Colloids Surfaces A Physicochem. Eng. Asp. 428 (2013) 100–110. https://doi.org/10.1016/j.colsurfa.2013.03.034.

[80] S.A. Muyibi, L.M. Evison, Optimizing physical parameters affecting coagulation of turbid water with Morninga oleifera seeds, Water Res. 29 (1995) 2689–2695. https://doi.org/10.1016/0043-1354(95)00133-6.

[81] Brazil, Portaria de Consolidação n°5 (National Consolidation Ordinance nº5), Brasilia, Brazil, 2017.

[82] M.M. Momeni, D. Kahforoushan, F. Abbasi, S. Ghanbarian, Using Chitosan/CHPATC as coagulant to remove color and turbidity of industrial wastewater: Optimization through RSM design, J. Environ. Manage. 211 (2018) 347–355. https://doi.org/10.1016/j.jenvman.2018.01.031.

[83] A.P. Black, J.E. Singley, G.P. Whittle, J.S. Maulding, Stoichiometry of the Coagulation of Color-Causing Organic Compounds With Ferric Sulfate, J. Am. Water Works Assoc. 55 (1963) 1347–1366. https://doi.org/10.1002/j.1551-8833.1963.tb01151.x.

[84] E. Krause, V.A. Ettel, Solubilities and stabilities of ferric arsenate compounds, Hydrometallurgy. 22 (1989) 311–337. https://doi.org/10.1016/0304-386X(89)90028-5.

[85] J.G. Hering, P.-Y. Chen, J.A. Wilkie, M. Elimelech, Arsenic Removal from Drinking Water during Coagulation, J. Environ. Eng. 123 (1997) 800–807. https://doi.org/10.1061/(ASCE)0733-9372(1997)123:8(800).

[86] J.E. Goodwill, X. Mai, Y. Jiang, D.A. Reckhow, J.E. Tobiason, Oxidation of manganese(II) with ferrate: Stoichiometry, kinetics, products and impact of organic carbon, Chemosphere. 159 (2016) 457–464. https://doi.org/10.1016/j.chemosphere.2016.06.014.

[87] Crystalquest, Ultrafiltration Systems & Membranes, (2020).

[88] M.J. Brandt, K.M. Johnson, A.J. Elphinston, D.D. Ratnayaka, Water Filtration, in:

Twort's Water Supply, Elsevier, 2017: pp. 367–406. https://doi.org/10.1016/B978-0-08-100025-0.00009-0.

[89] K. CHOO, H. LEE, S. CHOI, Iron and manganese removal and membrane fouling during UF in conjunction with prechlorination for drinking water treatment, J. Memb. Sci. 267 (2005) 18–26. https://doi.org/10.1016/j.memsci.2005.05.021.

[90] X. Du, F. Qu, H. Liang, K. Li, H. Yu, L. Bai, G. Li, Removal of antimony (III) from polluted surface water using a hybrid coagulation–flocculation–ultrafiltration (CF–UF) process, Chem. Eng. J. 254 (2014) 293–301. https://doi.org/10.1016/j.cej.2014.05.126.

[91] J. Roy, Economic benefits of arsenic removal from ground water — A case study from West Bengal, India, Sci. Total Environ. 397 (2008) 1–12. https://doi.org/10.1016/j.scitotenv.2008.02.007.

[92] A. Ahmad, P. van der Wens, K. Baken, L. de Waal, P. Bhattacharya, P. Stuyfzand, Arsenic reduction to <1 µg/L in Dutch drinking water, Environ. Int. 134 (2020) 105253. https://doi.org/10.1016/j.envint.2019.105253.

[93] T.R. Chowdhury, G.K. Basu, B.K. Mandal, B.K. Biswas, G. Samanta, U.K. Chowdhury, C.R. Chanda, D. Lodh, S.L. Roy, K.C. Saha, S. Roy, S. Kabir, Q. Quamruzzaman, D. Chakraborti, Arsenic poisoning in the Ganges delta, Nature. 401 (1999) 545–546. https://doi.org/10.1038/44056.

[94] L. Godo-Pla, P. Emiliano, S. González, M. Poch, F. Valero, H. Monclús, Implementation of an environmental decision support system for controlling the pre-oxidation step at a full-scale drinking water treatment plant, Water Sci. Technol. 81 (2020) 1778–1785. https://doi.org/10.2166/wst.2020.142.

[95] M.R. Moradi, A. Pihlajamäki, M. Hesampour, J. Ahlgren, M. Mänttäri, End-of-life RO membranes recycling: Reuse as NF membranes by polyelectrolyte layer-by-layer deposition, J. Memb. Sci. 584 (2019) 300–308. https://doi.org/10.1016/j.memsci.2019.04.060.

[96] E. Coutinho de Paula, M.C.S. Amaral, Extending the life-cycle of reverse

osmosis membranes: A review, Waste Manag. Res. 35 (2017) 456–470. https://doi.org/10.1177/0734242X16684383.

[97] Y. Zhang, H. Wang, Y. Li, B. Wang, J. Huang, S. Deng, G. Yu, Y. Wang, Removal of micropollutants by an electrochemically driven UV/chlorine process for decentralized water treatment, Water Res. 183 (2020) 116115. https://doi.org/10.1016/j.watres.2020.116115.

[98] M. Peter-Varbanets, C. Zurbrügg, C. Swartz, W. Pronk, Decentralized systems for potable water and the potential of membrane technology, Water Res. 43 (2009) 245–265. https://doi.org/10.1016/j.watres.2008.10.030.

[99] J. Hermia, Constant Pressure Blocking Filtration Laws - Application Topower-Law Non-Newtonian Fluids., Trans Inst Chem Eng. V 60 (1982) 183–187. https://doi.org/Constant pressure blocking filtration laws—application to power-law non-newtonian fluids.

[100] I. Vergili, Y. Kaya, U. Sen, Z.B. Gönder, C. Aydiner, Techno-economic analysis of textile dye bath wastewater treatment by integrated membrane processes under the zero liquid discharge approach, Resour. Conserv. Recycl. 58 (2012) 25–35. https://doi.org/10.1016/j.resconrec.2011.10.005.

[101] M.C. Dodd, N.D. Vu, A. Ammann, V.C. Le, R. Kissner, H.V. Pham, T.H. Cao, M. Berg, U. von Gunten, Kinetics and Mechanistic Aspects of As(III) Oxidation by Aqueous Chlorine, Chloramines, and Ozone: Relevance to Drinking Water Treatment, Environ. Sci. Technol. 40 (2006) 3285–3292. https://doi.org/10.1021/es0524999.

[102] C. Hu, H. Liu, G. Chen, J. Qu, Effect of aluminum speciation on arsenic removal during coagulation process, Sep. Purif. Technol. 86 (2012) 35–40. https://doi.org/10.1016/j.seppur.2011.10.017.

[103] D. Ellis, C. Bouchard, G. Lantagne, Removal of iron and manganese from groundwater by oxidation and microfiltration, Desalination. 130 (2000) 255–264. https://doi.org/10.1016/S0011-9164(00)00090-4.

[104] V. Pallier, G. Feuillade-Cathalifaud, B. Serpaud, J.-C. Bollinger, Effect of organic matter on arsenic removal during coagulation/flocculation treatment, J. Colloid Interface Sci. 342 (2010) 26–32. https://doi.org/10.1016/j.jcis.2009.09.068.

[105] Y.T. Hameed, A. Idris, S.A. Hussain, N. Abdullah, A tannin-based agent for coagulation and flocculation of municipal wastewater: Chemical composition, performance assessment compared to Polyaluminum chloride, and application in a pilot plant, J. Environ. Manage. 184 (2016) 494–503. https://doi.org/10.1016/j.jenvman.2016.10.033.

[106] Q. Feng, H. Kanoh, K. Ooi, Manganese oxide porous crystals, J. Mater. Chem. 9 (1999) 319–333. https://doi.org/10.1039/a805369c.

[107] W.H.O. WHO, Guidelines for Drinking-water Quality, Genebra, 2011. https://doi.org/10.1016/S1462-0758(00)00006-6.

[108] A.I. Schäfer, L.D. Nghiem, N. Oschmann, Bisphenol A retention in the direct ultrafiltration of greywater, J. Memb. Sci. 283 (2006) 233–243. https://doi.org/10.1016/j.memsci.2006.06.035.

[109] K. Touati, L. Gzara, S. Mahfoudhi, S. Bourezgui, A. Hafiane, H. Elfil, Treatment of coastal well water using ultrafiltration-nanofiltration-reverse osmosis to produce isotonic solutions and drinking water: Fouling behavior and energy efficiency, J. Clean. Prod. 200 (2018) 1053–1064. https://doi.org/10.1016/j.jclepro.2018.08.024.

[110] T. Ahmad, K. Ahmad, M. Alam, Sludge quantification at water treatment plant and its management scenario, Environ. Monit. Assess. 189 (2017) 453. https://doi.org/10.1007/s10661-017-6166-1.

1 APPENDIX A – COPYRIGHT CLEARANCE

CHAPTER 1. Theoretical background

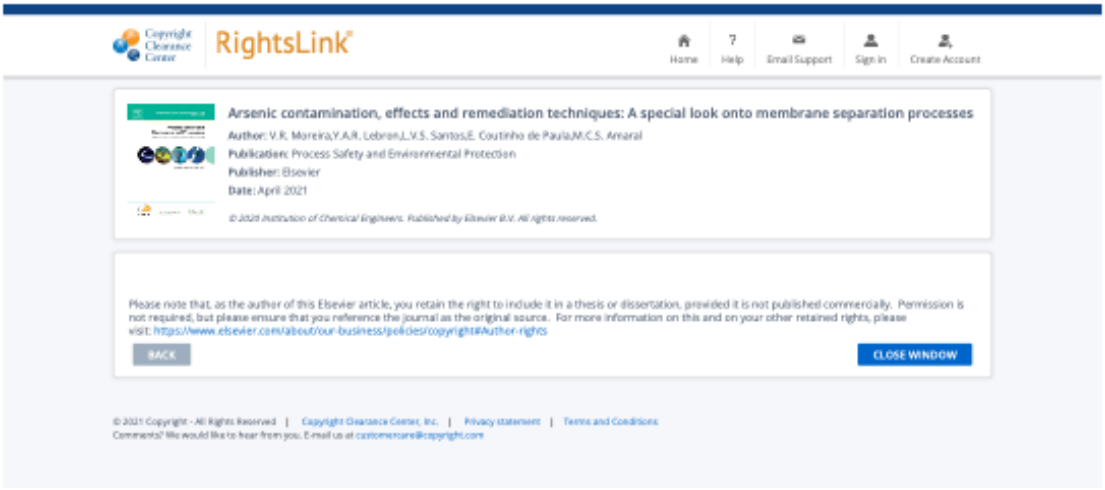

CHAPTER 2. Dead-end ultrafiltration as a cost-effective strategy for improving arsenic removal from high turbidity waters in conventional drinking water facilities

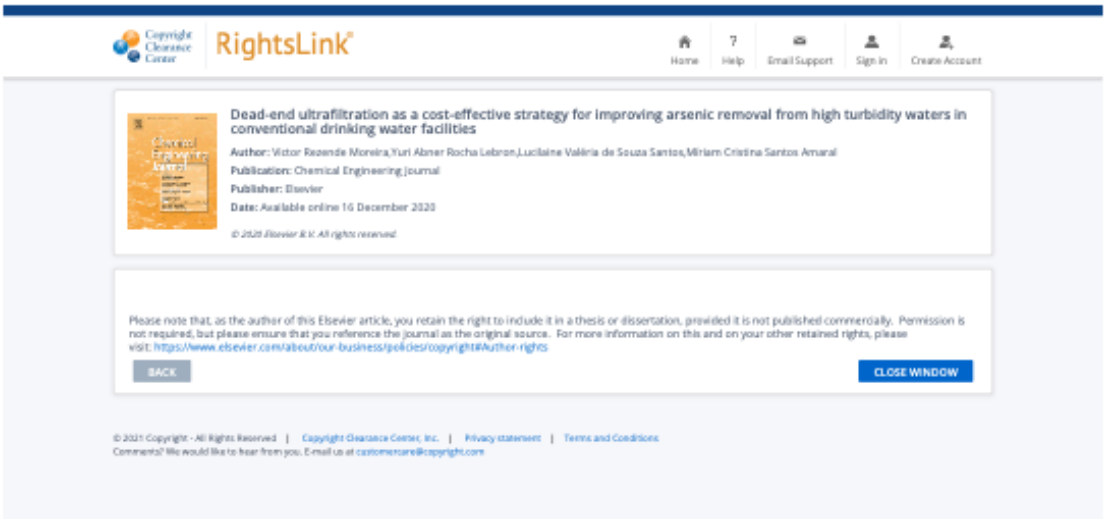

CHAPTER 3. Recycled reverse osmosis membrane combined with pre-oxidation for improved arsenic removal from high turbidity waters and retrofit of conventional drinking water treatment process

Recycled reverse osmosis membrane combined with pre-oxidation for improved arsenic removal from high turbidity waters and retrofit of conventional drinking water treatment process

Author:
Victor Rezende Moreira,Yuri Abner Rocha Lebron,Eduardo Coutinho de Paula,Lucilaine Valéria de Souza Santos,Miriam Cristina Santos Amaral

Publication: Journal of Cleaner Production

Publisher: Elsevier

Date: 20 August 2021